République Algérienne Démocratique et Populaire

Ministère de l'Enseignement Superieure et de la Recherche Scientifique

Université Echahid Hamma Lakhdar d'El-Oued

FACULTE DE TECHNOLOGIE

DEPARTEMENT DE GENIE MECANIQUE

Mémoire de fin d'étude

Présenté pour l'obtention du diplôme de

MASTER ACADEMIQUE

Domaine : Sciences et Technologies

Filière : Electromécanique

Spécialité : Electromécanique

Thème

High Performance Control of a Six-Phase Induction Machine Using Multilevel converters

Devant le jury composé de :

Dr Abdelkader Mahmoudi	Président
Dr Khaled Miloudi	Examinateur
Dr Hamza Mesai Ahmed	Encadreur

Présenté par :

- Selatna Hamza
- Selatna Hichem
- Hechifa Abdelhak

2023/2022

Remerciements

First of all, we thank Almighty God for giving us the strength and the will to carry out this work

We would like to thank our supervisor, ***Dr: Mesai Ahmed Hamza***

For his presence, the zeal with which he proposed and followed our project, and the valuable advice he gave us.

I would like to thank all the members of the jury for agreeing to judge this work.

It gives me particular pleasure to express here our gratitude to all those who have made this work possible.

Dedication

I dedicate this work

My dear parents in particular to my brothers

And my sisters Marwa, Abir and my niece Rowan

To Dr. Mesai Ahmed Hamza and Dr. Abd Moumen Hechifa and Dr. Ali Baboukha

For my whole family in general

To all my friends

Selatna Hamza

Dedication

I dedicate this work

To my dear parents in particular

To my brothers and sisters

To Dr. Mesai Ahmed Hamza and Dr. Abd Moumen Hechifa and Dr. Ali Baboukha

For all my family in general

To all my friends and in particular my friend Hatim

Selatna Hichem

Dedication

I dedicate this work

My dear parents in particular

To my brothers and sisters

To Dr. Mesai Ahmed Hamza

For all my family in general

To all my friends

Hechifa Abdelhak

Ddication

Remerciement

Summary

List of figures

List of tables

List of figures:

List of tables

SYMBOLS

- Modeling Parameters of 6PH-IM :

R_s	(Ω)	Stator resistance per phase,
R_r	(Ω)	Rotor resistance per phase,
L_s	(H)	Stator cyclic inductance by phase,
L_r	(H)	Rotor cyclic inductance per phase,
L_m	(H)	Mutual cyclic inductance (between stator and rotor), magnetizing inductance,
l_s	(H)	Specific inductance of a statoric phase,
l_r	(H)	Clean inductance of a rotor phase,
m_s	(H)	Mutual inductance between two stator phases,
m_r	(H)	Mutual inductance between two rotor phases,
M	(H)	Maximum value of mutual inductance between stator phase and other rotoric phase,
p	$(-)$	number of pole pairs,
C_{em}	(N.m)	Electromagnetic torque of the generator

- **Repere :**

(s_a, s_b, s_c)	Magnetic axes linked to three-phase stator windings,
(r_a, r_b, r_c)	Magnetic axes linked to three-phase rotor windings,
$(dq_1), (dq_2)$	Park reference axes,
$(\alpha\beta_1), (\alpha\beta_2)$	Concordia/Clarke reference axes,
θ_{sr} (rad)	Rotor angular position relative to stator,
θ_s (rad)	Stator angular position relative to axis (d).
θ_r (rad)	Rotor angular position relative to axis (d).

- Electrical quantities :

$v_{s\ abc1}, v_{s\ abc2}$	(V)	Three Phase Instantaneous Stator Voltages,
$v_{r\ a,\ b,\ c}$	(V)	Three Phase Instantaneous Stator Voltages,
$v_{s\ dq1},\ v_{s\ dq2}$	(V)	Two-phase stator voltages in landmark (d, q),
v_{rdq}	(V)	Two-phase stator voltages in landmark (d, q),
V_s	(V)	Stator Voltage Vector Module,
$i_{s\ abc1}, i_{s\ abc2}$	(A)	Three Phase Stator Instantaneous Currents,
$i_{r\ abc}$	(A)	Three Phase Stator Instantaneous Currents,
$i_{s\ dq1}$,$i_{s\ dq2}$	(A)	Two-phase stator currents in landmark (d, q),
i_{rdq}	(A)	Two-phase stator currents in landmark (d, q),
$\phi_{s\ abc1}, \phi_{s\ abc2}$	(Wb)	Instant Magnetic Flow to Stator,
$\phi_{s\ dq1},\ \phi_{s\ dq2}$	(Wb)	Two-phase stator flows in the rotating landmark (d, q).

Ψ_s	(Wb)	Stator flux vector module.
$\phi_{r\,ab\,c}$	(Wb)	Rotor magnetic flux vector,
ϕ_{rdq}	(Wb)	Two-phase rotor flows in the rotating landmark (d, q).
Ψ_r	(Wb)	Rotor Flux Vector Module.
P_s	(W)	Stator Active Power,
Q_s	(VAr)	Stator reactive power.
$P_{réseau}$	(W)	Power supplied to the network,

- Mechanical quantities **:**

ω_r	(rad/s)	Electric pulse corresponding to the speed of rotation,
ω_s	(rad/s)	Electric pulsation of stator quantities (rotating field),
G	(–)	Rotation speed shift,
f_s	(Hz)	Electrical frequency of stator quantities,
f_r	(Hz)	Electrical frequency of rotor quantities,
N_s	(tr/min)	Speed of the rotating field,

- **Transformations :**

s	Laplace operator,
$P\,(\theta)$	Park Transformation:$X_{sa,b,c} \rightarrow X_{sd,q}$ et$X_{ra,b,c} \rightarrow X_{rd,q}$,

- Control quantities of the 6PH-IM **:**

K_p, K_i	(–)	Proportional and integral components of the PI corrector,
r	(–)	Modulation rate (adjustment index),
m	(–)	modulation index,
f_r	(Hz)	reference frequency,
w_i	(–)	Weight vector
η_i	(–)	learning rate
ψ_i,ϕ_i,	(–)	vector-valued functions
P_i	(–)	Predicate error
H_i	(–)	Matrix gradient
Q_i, R_i	(–)	matrices de covariance
S	(–)	Fonction de limite
α, β	(–)	Constant values

NOTATIONS

6PH-IM	: Six phase induction machine.
MSC	: Machine Side Converter.
CVI	: Indirect Vector Control.
MCC	: Machine à Courant Continu.
PWM	: Pulse Width Modulation.
PI	: Proportional Integral.

AC	: Alternatif Current.
DC	: Direct Current.
FOC	: Field Oriented Control.
ANN	: Artificial Neural Networks.
RNN	: Recurrent Neural Networks.
EKF	: Extended KalmanFilter .
MPC	: Model Predictive Control
PCC	: Predictive Current Control
MB-PCC	: Model-Based Predictive Current Control
MF-PCC	: Model-Free Predictive Current Control
MPPT	: Maximum Power Point Tracking.
MLP	: Multi Layer Perceptron.
IGBT	: Insulated Gate Bipolar Transistor.
NPC	: Neutral Point Clamped.
WECS	: Wind Energy Conversion Systems.

General Introduction

AC machines powered by static converters are finding more and more applications in high-power industrial areas. However, switching frequency and performance are limited by limitations of power components. It is necessary to segment the power in order to allow the use of components with higher switching frequency and to ensure an electric motor for high power applications, such as rail traction or naval propulsion, for example. One solution is to use multi-phase machines or multi-star machines to do this. The six phase induction machine is an example of this type of structure.

When using multiphase induction machines with more than three phases powered by one or more converters, power segmentation is an appropriate solution. Multiphase machines have advantages over their three-phase counterparts, such as lower nominal current per phase, higher torque density, higher ripples, etc.

Multiphase machines (the number of phases is greater than three) appeared in the 1920s for power segmentation of generators. These machines are set to gain a significant place in the field of variable speed drives for power, and thus especially for applications where low frequency ripples are required [1]. It is possible to remain in operation in single mode when a winding or component is placed in default.

For this reason, multiphase machines are increasingly used for some high-power industrial applications such as rail traction, ship propulsion and wind energy systems. Among these multi-phase drives, the asynchronous six-phase machines (6PH-IM).

Many studies have long been carried out on the six-phase induction machine (6PH-IM), also known as asynchronous double stator machine. It has the advantage of being robust, reliable and not very effective in degraded operation. Unfortunately, it has a major drawback: its dynamic structure is strongly non-linear and internal variables such as electromagnetic torque and rotor flux are strongly coupled. This makes the control of this machine complex. This thesis is organized into four chapters as follows:

The first chapter summarizes the latest developments concerning independent systems and different types of machines, in particular the multiphase machines to which the two-star asynchronous machine (6PH-IM) which is the subject of our work belongs.

In the second chapter, we present in the first part the modeling of the double star asynchronous machine with its power supply (two PWM controlled voltage inverters), in

the second part, the rotary flux control is applied to the 6PH-IM, present the system behavior under ordinary operating conditions then adverse conditions present internal parametric variations and external disturbances.

In Chapter II, we propose 6PH-IM modeling and various parts of our system (converter, continuous support) To do this, a number of simplified assumptions are used by modifying the baseline through the fleet conversion application to reduce collusion in the system and facilitate its equivalence.

The third chapter is dedicated to vector control by orientation of the rotor flux of the 6PH-IM. An overview of the vector control principle and a reminder of its different methods are presented. We then move to the application of the indirect method of the 6PH-IM. In which, Simulation results and interpretations to characterize the performance of the proposed method is presented. We end with a general conclusion.

In the last chapter, we will study the control performance of the machine based on multi-level inverters.

Finally, a general conclusion will summaries the most important points of this thesis.

Chapter I

Multiphase systems: state of the art, problematic and work context

I.1 Introduction :

Amongst many types of electrical motors, induction motors still enjoy the same popularity as they did a century ago. Several factors which include robustness, low cost and low maintenance have made them popular for industrial applications when compared to dc and other ac motors. Another aspect in induction motor drives which has been researched recently is the use of multiphase induction motors where the number of stator phases is more than three.

In this chapter, we will first present the history of electrical machines. Next, we will define the multi-phase machines and give a general description of their characteristics working principle and their advantages and disadvantages of this machine in different application Finally, an overview of multi-level converter fed the six phase induction machine is proposed.

I.2 General information on the machines:

I.2.1 History of electric machines:

In 1811 the English human Michael Faraday produced the first electromagnetic motor, and in 1822 Peter Barlow added a toothed wheel.

In 1831 Faraday stated the principles of electromagnetic induction. In parallel, the Russian Friedrich Emil Lenz and the American Joseph Henry have carried out similar work, thus contributing to the discovery and understanding of this phenomenon. The following year Ampere, in collaboration with the French manufacturer Hippolyte Paxi, produced the direct current generator In 1836 the Englishman Hyade Clarke produced a machine whose structure was reversed from that of Paxi/Ampère which improved the rectifier switch.

In 1842 Davidson uses one of the first rotating motors with variable reactance.

In 1848, Froment engines appeared, with a torque of 500 N.m. These motors were used for industrial applications.

In 1860 the company “l'Alliance” industrially manufactured generators of complex structures.

In 1865 the Italian Antonio Pacinotti built a prototype of a direct current machine with ring armature and radial commutator, the operation of which was greatly improved.

In 1888 Nikola Tesla invented the first alternating current motor, which had a major role in the development of the electrical industry.

In 1889 the German Michael Dolivo-Dobrowolski produced the first three-phase asynchronous machine, which largely dominated the field of electrical machines, thanks to several advantages it had over other types. It is the simplest to manufacture, the least expensive, the least demanding in terms of maintenance, has a very low failure rate, manufactured in large quantities and in a very large scale of powers, etc.

Since the end of the 1920s, machines with two three-phase stator windings had been introduced to increase the power of very high-power synchronous alternators[1].

I.2.2 Classification of electrical machines

The classification of machines can be done in several ways:

- According to the way of supplying or delivering the current/voltage.
- According to the construction.

I.2.3 Depending on the type of food

- Direct Current Machines.
- DC machines either series, parallel or compound.
- Alternating current machines.
- Synchronous machines.

I.2.4 Synchronous machines.

According to their construction.

- Asynchronous machines.
- Machines without collector.
- Permanent magnet synchronous machine.
- Machines with manifold.
- DC machines.

In addition, multiphase machines (whose number of phases is more than three) appeared in the years1920 for alternator power segmentation[2].

I.3 State of the art of multiphase induction machine:

I.3.1 Structure des machines multi phase :

We can classify the machines according to several ways either by its way of feeding (way of delivering the current/voltage) or by its construction. The machine can be asynchronous with wound rotor, with squirrel cage or synchronous with permanent magnets, with excitation windings, with smooth poles or with salient poles, with or without dampers. These machines can be powered by current switches or voltage inverters. Multi-phase machines, as its name suggests, behave like the classic three-phase asynchronous machine two parts: [3]

- A rotating part with a solid cylindrical shape on a shaft is the rotor which is built from windings connected to themselves:
- A stationary part with a hollow cylindrical shape is the stator which comprises several three-phase windings, magnetically coupled orotherwise, and whose respective phases are grouped into several stars. Each star is powered by its own static converter.

I.4 The characteristics of multi-phase machines:

According to the number of phases that we can have in the stator (the stator phases) which is or multiple name of three, we distinguish two types of type 1 multi-phase machines" are called "multi-phase machines " and "type 2 multi-phase machines". Moreover, one rarely considers the or the number of phases is an even number except if this one is a multiple of three [4].

There can be several possible configurations in a machine with a given number of phases depending on the angular offset α between two adjacent coils. That is to say the offset between the stars. To be able to differentiate between the possible configurations, another term can be introduced: the number of equivalent phases, it is defined as follows:

$$npha = \frac{\pi}{a} \qquad \text{(I.1)}$$

For example: 6phase induction machine (6phase) , with angular offset between the stars $a = \frac{\pi}{6}$ has characteristics different from those of a machine having the same number of phases but their stars are shifted by $a = \frac{\pi}{3}$

I.4.1 Type 1 multi-phase machines:

In this type of machine the number of stator phases is a multiple of three, they can be grouped into η star, three-phase [4].

$$nph = 3\eta \ (\eta = 1,2,3\ldots.) \qquad (I.2)$$

Taple.1: machines whose number of stator phases is a multiple of three "type1"

Number of phases (q)	Phase equivalent number (qa)	Angular offset (a)	Schematic representation, position of the coils
3	**3**	$\frac{\pi}{3}$	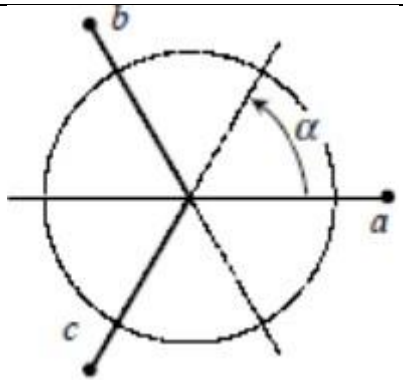
6	**3**	$\frac{\pi}{3}$	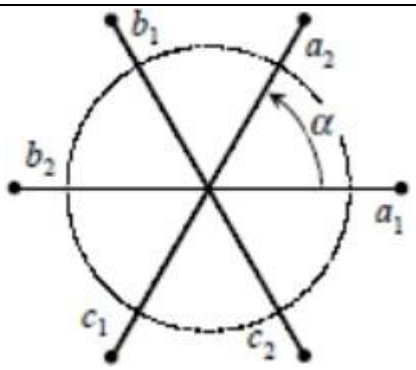
6	**6**	$\frac{\pi}{6}$	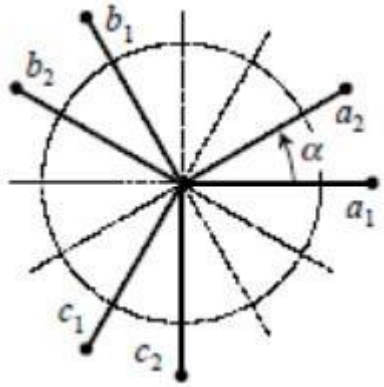

9	**9**	$\frac{\pi}{9}$	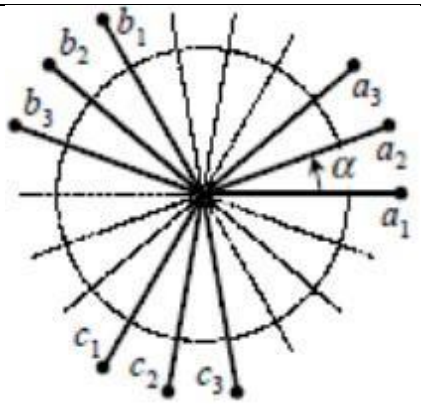
12	**6**	$\frac{\pi}{6}$	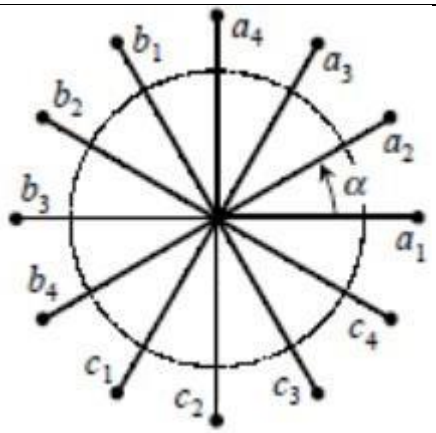
12	**12**	$\frac{\pi}{12}$	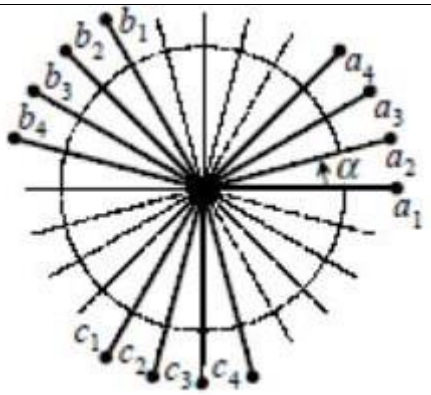

I.4.2 Type 2 multiple machines:

Type 2 multiple machines with an odd number of stator phases (nph).

$$nph = 3\eta+1 \ (\eta = 1,2,3\ldots.) \qquad \text{(I.3)}$$

For the angular shift α between two adjacent coils, the phases of which are shifted regularly from $2a = \frac{2\pi}{nph}$ So we have $nph = nph_a = \frac{\pi}{a}$ (I.4)

Table.I.2: machines whose number of stator phases is an odd number ''type2''.

Number of phases (q)	Phase equivalent number (qa)	Angular offset (a)	Schematic representation, position of the coils
5	**5**	$\frac{\pi}{5}$	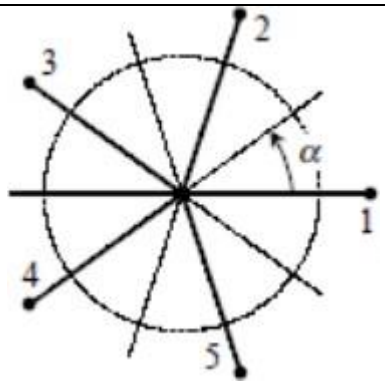
7	**7**	$\frac{\pi}{7}$	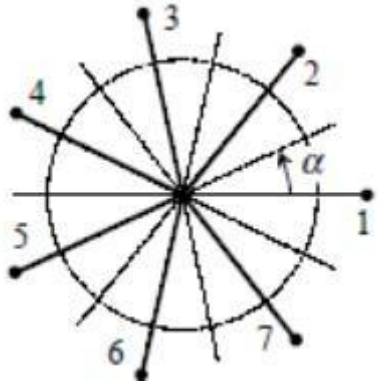
9	**9**	$\frac{\pi}{9}$	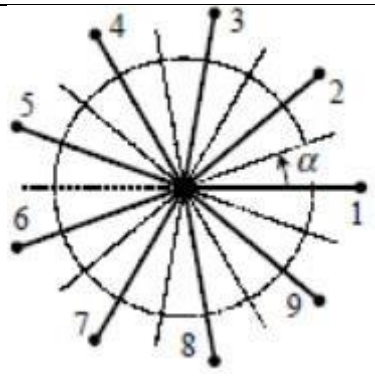

11	**11**	$\frac{\pi}{11}$	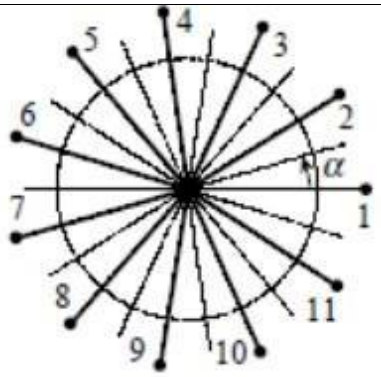
13	**13**	$\frac{\pi}{13}$	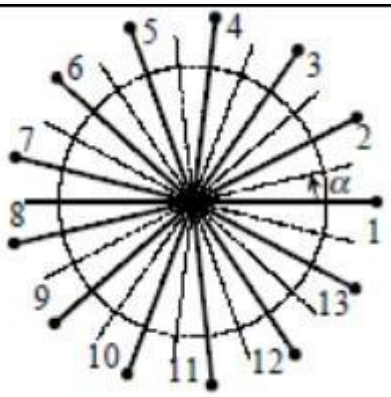

I.5 Operating principle of the multi-phase machine

Taking the six phase induction machine as an example: [5].

The stator currents create a rotating magnetic field in the two stators (star 1 powered by three-phase currents and star powered by the same three-phase currents but shifted by an angle α). The rotational frequency of this field is imposed by the frequency of the stator currents, i.e. its rotational speed is proportional to the frequency of the electrical power supply, the speed of this rotating field is called synchronism speed. It defines as follows[4].

$$w_s = \frac{t_s}{p}[rad/s] \qquad \text{(I.5)}$$

These two rotating fields produced by the two stator windings will induce currents in the conductors of the rotor. Thus generating emfs that will cause the rotor to spin at a speed ωr less than that of synchronism ($\omega r < \omega s$), thus the effects of stator induction on rotor induced currents manifest as the development of an electromagnetic force couple on the rotor such that the speed difference is reduced. The speed difference between the rotor and the stator field is called relative speed :

$$\omega = \omega_s - \Omega \qquad \text{(I.6)}$$

We will then say that these two fields slip with respect to the rotor and we define this slip by the ratio:

$$g = \frac{w}{w_s} = \frac{w_s - \Omega}{w_s} \qquad (I.7)$$

The different operating modes depend on the value of the slip:

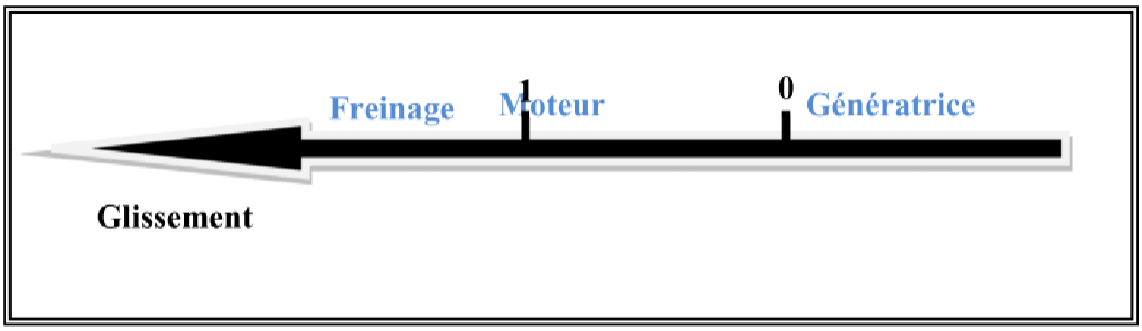

Figure I.1 : Operating modes according to slip

I.5.1 Advantages of Multiphase Machines:

Multiphase machines have subsequently attracted growing interest, and in particular the six phase induction machine (6PH-IM), which in addition to the advantages of three-phase [6]. cage asynchronous machines, those of multiphase machines. Indeed, multi-phase drives have several advantages over conventional machines.

- Power segmentation.
- Improved reliability.
- Reduction of harmonic currents.
- Improved power factor.
- Minimization of torque ripples and rotor losses.

I.5.2 Disadvantages of multi-phase machines:

However, the asynchronous machine has disadvantages such as [7] :

- ✓ The number of semiconductors increases with the number of phases, which may eventually increase the cost of the converter-machine assembly.
- ✓ The multiplication of the number of semiconductors with the dynamic structure is strongly nonlinear and the existence of a strong coupling between the torque and the flux, which obviously complicates its control.
- ✓ The major drawback of double star machines is the appearance of circulating harmonic currents when powered by a voltage inverter.

In our work we are interested in the six-phase machine

I.6 Six-phase "double star" machine models in the literature

The control of multi-phase machines is generally an extension of the control principles used for three-phase machines. As in the case of a three-phase machine, the control of a multi-phase machine is based on an appropriate machine model. In the particular case of a six-phase machine, two different models have been commonly used for the development of the control, namely the double-dq] model and the VSD model. For the double-dq model, two separate three-phase decoupling (Clarke) transformations are first applied to the two sets of energy and to the two sets of three-phase windings. Taking stator currents as an example, we get two pairs of α-β currents($i_{\alpha 1}$ $-i_{\beta 1}$and $i_{\alpha 2}$ $-i_{\beta 2}$) in the stationary frame. These currents are then subjected to a rotation transformation (Park), to give two pairs. corresponding d-q currents (i_{d1} i_{q1} et i_{d2} i_{q2}). Since the d axis is aligned with the rotor flux, the machine flux is controlled by regulating id1 and id2, while the machine torque is controlled by regulating iq1 and iq2. This is analogous to rotor flux-oriented control (RFOC) in three-phase machines, except that two sets of d-q current controllers are required instead of just one.

An implementation of current control based on this approach has been reported in An extension of this model to a nine-phase machine has been demonstrated in for an ultra-high-speed elevator application, using three decoupling transformations instead of two and three pairs of d-q current controllers. However, an obvious disadvantage of this model is that its application is limited to multiphase machines with several three-phase windings. An alternative to the double-dq model is the VSD model developed in[9]. The VSD model is an important tool for the analysis of polyphone machines and, subsequently, for the development of current control methods. Using the VSD approach, an n-phase machine can be represented using n/2 (or (n-1)/2 for machines with an odd number of phases) orthogonal subspaces, innate an α-β subspace and several x-y subspaces, as well as the homopolar components. For a machine with a sinusoidal magneto motive force (MMF) distribution, only the α-β components contribute to the useful conversion of electromechanical energy, while the x-y and zero-sequence components only produce losses. Based on the VSD approach, the α-β equations of a polyphone machine are identical to those of a three-phase machine, so the direct implementation of standard three-phase vector control becomes possible. Nevertheless, due to the presence of additional loss-producing components, the corresponding currents must also be controlled to improve system performance. Compared to the double-dq model, the VSD model is more general and is applicable to polyphone

machines of any number of phases. The separation of flux and torque producing components (α-β) from loss producing components (x-y and zero-sequence) in the VSD model provides an insightful tool for the development of spatial vector pulse width modulation (SVPWM) for multiphase machines, which cannot be done easily using the double-dq model. In terms of control, it was concluded that similar dynamic performance can be obtained regardless of the type of model chosen. Nevertheless, it has also been noted in that six-phase machine vector control using the VSD approach requires voltage decoupling terms that are less complicated than in the double-dq approach. It should be noted that although the VSD and double-dq models are essentially applicable to the same machine, the machine parameters for each model are different. In, it has been shown that if the mutual leakage inductance between the two three-phase windings is considered negligible, a simple and direct correlation between the parameters of the two models exists. The stator resistance and stator leakage inductance are equal for both models, while the mutual inductance, rotor leakage inductance and rotor resistance of the VSD model are twice that of the dual model -dq. Despite the various advantages of the VSD model, the variables are more difficult to physically interpret, unlike the double-dq model where dq1 is clearly tied to the first set of "star 1" windings and dq2 to the second set of "star 2" windings . Due to this advantage, the double-dq model is the model adopted in this work[8].

I.7 Works carried out for the control of the six-phase asynchronous machine

There are several control techniques have been studied to control the asynchronous machine. They have been developed to replace vector control, such as direct torque control DTC and Sliding Mode Control and Sliding Mode Control SMC, providing good robustness against parameters variations. Among the techniques applied to the control of the asynchronous machine, the following:

- ✓ Vector Command; Study and Control of a Double Star Asynchronous Machine for DJABOREBBI Amina 2013. However, producing a speed control for this machine is of interest.
- ✓ Vector Command; High performance controls of a MADE double star asynchronous machine via multi-level converters for Mr. Mesai Ahmed Hamza 2019. The main objective of this work is to present solutions to improve the performance and increase the control reliability of the machine. dual star asynchronous (6PH-IM).
- ✓ direct torque control DTC; Contribution to the Control of the Double Star Synchronous Machine for LAGGOUN Louanasse 2019. the study and improvement

of the performance of the direct torque control (DTC) of a permanent magnet double star synchronous machine (6PHIMAP) powered by two inverters Of voltage.

- ✓ direct torque control DTC; Contribution to the Control of a Double Star Asynchronous Machine for Brahim KIYYOUR 2020. The aim is to improve the performance of the Direct Torque Control (DTC) applied to this.
- ✓ Sliding Mode Control; contribution to the control of the double star asynchronous machine for AMIMEUR HOCINE 2012. contribute to the control of this electric machine.
- ✓ Sliding Mode Control of the Double Star Asynchronous Machine for SOUSSA CHEMS EDDINE and WALID ABADI and HOUCINE GABOUSSA and ABDELDGALIL HECHIFA 2022. In this thesis we have adopted PI regulators in vector control by flux orientation.

I.8 Multilevel converters in the literature

Multilevel converters are finding increased attention in industry application as one of the preferred choices of electronic power conversion for high-power applications [9] [10] [11] [12] [13] [14] [15] [16] [17] [18] .They have successfully made their way into the industry and therefore can be considered a mature and proven technology. Currently, they are commercialized in standard and customized products hat power a wide range of applications, such as compressors, extruders, pumps, fans, grinding mills, rolling mills, conveyors, crushers, blast furnace blowers, gas turbine starters, mixers, mine hoists, reactive power compensation, marine propulsion, high-voltage direct-current (HVDC) transmission, hydro pumped storage, wind energy conversion, and railway traction, to name a few [9]–[18]. Converters for these applications are commercially offered by a growing group of companies in the field [19]-[26]. Although it is an enabling and already proven technology, multilevel converters present a great deal of challenges, and even more importantly, they offer such a wide range of possibilities that their research and development is still growing in depth and width. Researchers all over the world are contributing to further improve energy efficiency, reliability, power density, simplicity, and cost of multilevel converters, and broaden their application field as they become more attractive and competitive than classic topologies. Recently, many publications have addressed multilevel converter technology and stressed the growing importance of multilevel converters for high-power applications [12]–[17]. These works have a survey

and tutorial nature and cover in depth traditional and well-established multilevel converter topologies, such as the neutral point clamped (NPC), cascaded H-bridge (CHB), and flying capacitor (FC), as well as the most used modulation methods. In this thesis an application of three and five level converters fed the six phase induction machine is presented in chapter 4.

I.9 Conclusion

In this chapter a state of the art relating to the history of the electric machines with their constitutions and operating principles, such as the existing topologies, the model types and the various strategies of controls most for the multiphase systems is presented. The advantages and disadvantages of each strategy have been addressed using the work already carried out by several researchers concerning the various control techniques most used in multiphase systems.

The next chapter will present the modeling and the vector control of the six-phase asynchronous machine powered by two voltage inverters.

CHAPTER II

Study and modeling of the six-phase Induction machine

II.1 introduction

The modeling of any system is necessary for the application of a particular command. In this chapter, we will be interested in the modeling of the different parts of the studied system, which consists of the 6PH-IM, the converters and the continuous bus. in fact the modeling of the electrical machine calls upon very complex equations , the distribution of the windings and the specific geometry of the 6PH-IM make its model difficult to implement. However, the adoption of certain simplifying assumptions makes it possible to circumvent this difficulty. In this chapter, the modeling of 6PH-IM feed by two power converters and are presented,

In this study an angular offset of the 6 PH-IM $\alpha = 30^\circ$ (Angle between adjacent phases) is considered. Finally, simulation results will be presented and commented on.

II.2 Six phase machine description:

The 6PH-IM consists of a stator carrying two identical three-phase windings offset by an electrical angle $\alpha = 30^\circ$, and a squirrel-cage rotor. Figure 2.1 schematically represents the windings of the 6PH-IM. The angles θr and $(\theta r - \alpha)$ respectively represent the position of the rotor (phase ar) with respect to star 1 (phase as1) and star 2 (phase as2). The quantities relating to the two stars (1 and 2) will be denoted respectively by the indices 1 and 2 [27].

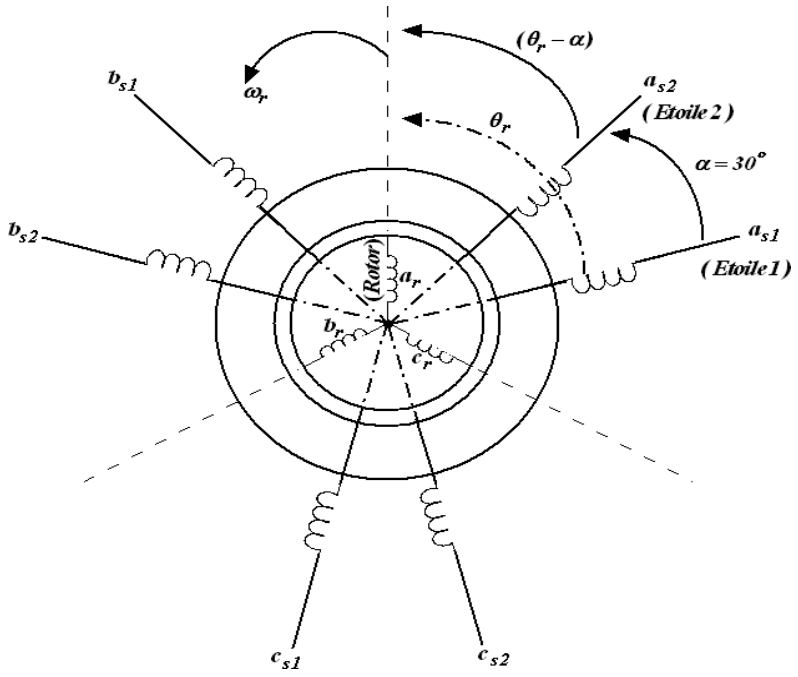

FigureII.1 : Schematic representation of the 6PH-IM windings

II.3 Simplifying assumptions:

6PH-IM, with the distribution of its windings and its own geometry is very complex to lend itself to an analysis taking into account its exact configuration, and as we have already raised, it is then necessary to adopt some simplifying assumptions, [28].

We consider the following assumptions:

- The magnetic circuit is unsaturated, which makes it possible to express the fluxes as linear functions of the currents.
- Losses (by hysteresis and eddy current) are neglected. the magneto motive forces created by each of the phases of the two armatures have a sinusoidal distribution.
- The effect of the temperature variation on the stator and rotor resistances is negligible.
- The perfect symmetry of the machine, both magnetic and electric.
- The air gap is constant.
- Neglected skin effect.

II.4 Modeling of the six-phase machine[8]:

II.4.1 Electrical equation of the six-phase machine:

The voltage equations of the machine six phase represent for each winding the sum of the holmic drop and the inductive drop due to the flux.

For star 1:

$$\begin{cases} U_{as1} = R_{s1} i_{as1} + \dfrac{d\varphi_{as1}}{dt} \\ U_{bs1} = R_{s1} i_{bs1} + \dfrac{d\varphi_{bs1}}{dt} \\ U_{cs1} = R_{s1} i_{cs1} + \dfrac{d\varphi_{cs1}}{dt} \end{cases} \quad \text{(II.1)}$$

For star 2:

$$\begin{cases} U_{as2} = R_{s2} i_{as2} + \dfrac{d\varphi_{as2}}{dt} \\ U_{bs2} = R_{s2} i_{bs2} + \dfrac{d\varphi_{bs2}}{dt} \\ U_{cs2} = R_{s2} i_{cs2} + \dfrac{d\varphi_{cs2}}{dt} \end{cases} \quad \text{(II.2)}$$

For rotor:

$$\begin{cases} 0 = U_{ar} = R_r i_{ar} + \dfrac{d\varphi_{ar}}{dt} \\ 0 = U_{br} = R_r i_{br} + \dfrac{d\varphi_{br}}{dt} \\ 0 = U_{cr} = R_r i_{cr} + \dfrac{d\varphi_{cr}}{dt} \end{cases} \quad \text{(II.3)}$$

In matrix form, we have:

For star 1: $[U_{s1}] = [R_{s1}][i_{s1}] + \dfrac{d}{dt}[\varphi_{s1}]$ (II.4)

For star 2: $[U_{s2}] = [R_{s2}][i_{s2}] + \dfrac{d}{dt}[\varphi_{s2}]$ (II.5)

For rotor: $[U_r] = [R_r][i_r] + \dfrac{d}{dt}[\varphi_r]$ (II.6)

With :

$$[U_{s1}] = \begin{bmatrix} U_{as1} \\ U_{bs1} \\ U_{cs1} \end{bmatrix} ; [U_{s2}] = \begin{bmatrix} U_{as2} \\ U_{bs2} \\ U_{cs2} \end{bmatrix} ; [U_r] = \begin{bmatrix} U_{ar} \\ U_{br} \\ U_{cr} \end{bmatrix} \quad \text{(II.7)}$$

$[U_{s1}]$: Star 1 voltage matrix ;

$[U_{s2}]$: Star 2 voltage matrix;

$[U_r]$: Rotor Voltage Matrix.

With :

$$[i_{s1}] = \begin{bmatrix} i_{as1} \\ i_{bs1} \\ i_{cs1} \end{bmatrix} ; [i_{s2}] = \begin{bmatrix} i_{as2} \\ i_{bs2} \\ i_{cs2} \end{bmatrix} ; [i_r] = \begin{bmatrix} i_{ar} \\ i_{br} \\ i_{cr} \end{bmatrix} \quad \text{(II.8)}$$

$[i_{s1}]$:Current matrix of star 1;

$[i_{s2}]$: Current matrix of star 2;

$[i_r]$: Rotor current matrix.

With :

$$R_{as1} = R_{bs1} = R_{cs1} \; ; \; R_{as2} = R_{bs2} = R_{cs2} \text{ et } R_{ar} = R_{br} = R_{cr} \tag{II.9}$$

$$[R_{s1}] = \begin{bmatrix} R_{as1} & 0 & 0 \\ 0 & R_{bs1} & 0 \\ 0 & 0 & R_{cs1} \end{bmatrix} ; \quad [R_{s2}] = \begin{bmatrix} R_{as2} & 0 & 0 \\ 0 & R_{bs2} & 0 \\ 0 & 0 & R_{cs2} \end{bmatrix} ; [R_r] = \begin{bmatrix} R_{ar} & 0 & 0 \\ 0 & R_{br} & 0 \\ 0 & 0 & R_{cr} \end{bmatrix} \tag{II.10}$$

$[R_{s1}]$:Resistance of a star phase 1;

$[R_{s2}]$: Resistance of a phase of star 2;

$[R_r]$: Resistance of a phase of the rotor.

$$[\varphi_{s1}] = \begin{bmatrix} \varphi_{as1} \\ \varphi_{bs1} \\ \varphi_{cs1} \end{bmatrix} ; [\varphi_{s2}] = \begin{bmatrix} \varphi_{as2} \\ \varphi_{bs2} \\ \varphi_{cs2} \end{bmatrix} ; [\varphi_r] = \begin{bmatrix} \varphi_{ar} \\ \varphi_{br} \\ \varphi_{cr} \end{bmatrix} \tag{II.11}$$

$[\varphi_{s1}]$: Flux matrix of star 1;

$[\varphi_{s2}]$: Flux matrix of star 2;

$[\varphi_r]$: Rotor flux matrix.

II.4.2 Magnetic equations of the six-phase machine:

The stator and rotor fluxes as a function of the currents, the self-inductances and the mutual inductances, are expressed from the matrix obtained by the following equations :

$$[L(\theta)] = \begin{bmatrix} [L_{s1,s1}] & [M_{s1,s2}] & [M_{s1,r}] \\ [M_{s2,s1}] & [L_{s2,s2}] & [M_{s2,r}] \\ [M_{r,s1}] & [M_{r,s2}] & [L_{r,r}] \end{bmatrix} \tag{II.12}$$

$$\begin{bmatrix} [\varphi_{s1}] \\ [\varphi_{s2}] \\ [\varphi_r] \end{bmatrix} = [L(\theta)] \cdot \begin{bmatrix} [i_{s1}] \\ [i_{s2}] \\ [i_r] \end{bmatrix} \tag{II.13}$$

The sub-matrices of the inductance matrix are expressed as follows:

$$[L_{s1,s1}] = \begin{bmatrix} (L_{s1} + L_{ms}) & L_{ms}\cos\left(\frac{2\pi}{3}\right) & L_{ms}\cos\left(\frac{4\pi}{3}\right) \\ L_{ms}\cos\left(\frac{4\pi}{3}\right) & (L_{s1} + L_{ms}) & L_{ms}\cos\left(\frac{2\pi}{3}\right) \\ L_{ms}\cos\left(\frac{2\pi}{3}\right) & L_{ms}\cos\left(\frac{4\pi}{3}\right) & (L_{s1} + L_{ms}) \end{bmatrix} \tag{II.14}$$

$$\left[L_{s2,s2}\right]=\begin{bmatrix} (L_{s2}+L_{ms}) & L_{ms}\cos\left(\frac{2\pi}{3}\right) & L_{ms}\cos\left(\frac{4\pi}{3}\right) \\ L_{ms}\cos\left(\frac{4\pi}{3}\right) & (L_{s2}+L_{ms}) & L_{ms}\cos\left(\frac{2\pi}{3}\right) \\ L_{ms}\cos\left(\frac{2\pi}{3}\right) & L_{ms}\cos\left(\frac{4\pi}{3}\right) & (L_{s2}+L_{ms}) \end{bmatrix} \quad \text{(II.15)}$$

$$\left[L_{r,r}\right]=\begin{bmatrix} (L_{r}+L_{mr}) & L_{mr}\cos\left(\frac{2\pi}{3}\right) & L_{mr}\cos\left(\frac{4\pi}{3}\right) \\ L_{mr}\cos\left(\frac{4\pi}{3}\right) & (L_{r}+L_{mr}) & L_{mr}\cos\left(\frac{2\pi}{3}\right) \\ L_{mr}\cos\left(\frac{2\pi}{3}\right) & L_{mr}\cos\left(\frac{4\pi}{3}\right) & (L_{r}+L_{mr}) \end{bmatrix} \quad \text{(II.16)}$$

$$\left[M_{s1,s2}\right]=\begin{bmatrix} L_{ms}\cos(\alpha) & L_{ms}\cos\left(\alpha+\frac{2\pi}{3}\right) & L_{ms}\cos\left(\alpha+\frac{4\pi}{3}\right) \\ L_{ms}\cos\left(\alpha+\frac{4\pi}{3}\right) & L_{ms}\cos(\alpha) & L_{ms}\cos\left(\alpha+\frac{2\pi}{3}\right) \\ L_{ms}\cos\left(\alpha+\frac{2\pi}{3}\right) & L_{ms}\cos\left(\alpha+\frac{4\pi}{3}\right) & L_{ms}\cos(\alpha) \end{bmatrix} \quad \text{(II.17)}$$

$$\left[M_{s1,r}\right]=\begin{bmatrix} L_{sr}\cos(\theta_r) & L_{sr}\cos\left(\theta_r+\frac{2\pi}{3}\right) & L_{sr}\cos\left(\theta_r+\frac{4\pi}{3}\right) \\ L_{sr}\cos\left(\theta_r+\frac{4\pi}{3}\right) & L_{sr}\cos(\theta_r) & L_{sr}\cos\left(\theta_r+\frac{2\pi}{3}\right) \\ L_{sr}\cos\left(\theta_r+\frac{2\pi}{3}\right) & L_{sr}\cos\left(\theta_r+\frac{4\pi}{3}\right) & L_{sr}\cos(\theta_r) \end{bmatrix} \quad \text{(II.18)}$$

$$\left[M_{s2,r}\right]=\begin{bmatrix} L_{sr}\cos(\theta_r-\alpha) & L_{sr}\cos\left(\theta_r-\alpha+\frac{2\pi}{3}\right) & L_{sr}\cos\left(\theta_r-\alpha+\frac{4\pi}{3}\right) \\ L_{sr}\cos\left(\theta_r-\alpha+\frac{4\pi}{3}\right) & L_{sr}\cos(\theta_r-\alpha) & L_{sr}\cos\left(\theta_r-\alpha+\frac{2\pi}{3}\right) \\ L_{sr}\cos\left(\theta_r-\alpha+\frac{2\pi}{3}\right) & L_{sr}\cos\left(\theta_r-\alpha+\frac{4\pi}{3}\right) & L_{sr}\cos(\theta_r-\alpha) \end{bmatrix} \quad \text{(II.19)}$$

$$\left[M_{s2,s1}\right]=\left[M_{s1,s2}\right]^t \;;\; \left[M_{r,s1}\right]=\left[M_{s1,r}\right]^t \;;\; \left[M_{r,s2}\right]=\left[M_{s2,r}\right]^t \quad \text{(II.20)}$$

$$L_{ms}=L_{mr}=L_{sr}=\frac{2}{3}L_m \quad \text{(II.21)}$$

With :

L_{s1} :The self-inductance of the stator1;

L_{s2} : The self-inductance of the stator2;

L_r : The self-inductance of a phase of the rotor;

L_{ms} : The maximum value of the stator mutual inductance coefficients;

L_{mr} : The maximum value of the rotor mutual inductance coefficients;

L_{sr} : The maximum value of the mutual inductance coefficients between a star and the rotor.

II.4.3 Magnetic energy of the six-phase machine:

We can calculate the magnetic energy stored in the rotor from the following expression.

$$w_{mag} = \frac{1}{2}\left([i_{s1}]^t[\varphi_{s1}] + [i_{s2}]^t[\varphi_{s2}] + [i_r]^t[\varphi_r]\right) \quad \text{(II.22)}$$

II.4.4 Expression of the electromagnetic torque of the six-phase machine:

The expression of the electromagnetic torque is obtained by the derivation of the co energy with respect to the magnetic angle .

$$C_{em} = \frac{d}{d\theta_{mag}} w_{mag} = p\frac{d}{d\theta_e} w_{mag} \quad \text{(II.23)}$$

With :

p : pole pair number.

θ_{mag} : magnetic angle.

θ_e : electric angle

$$C_{em} = \frac{p}{2}\left([i_{s1}]\frac{d}{d\theta_r}[L_{s1,r}][i_r]^t + [i_{s2}]\frac{d}{d\theta_r}[L_{s2,r}][i_r]^t\right) \quad \text{(II.24)}$$

With :

θ_r : Rotor position relative to star 1 [rd].

II.4.5 Mechanical equation of the six-phase machine:

$$J\frac{d\Omega}{dt} = C_{méc} = C_g - C_{em} - C_f \tag{II.25}$$

With :

$$\Omega = \frac{\omega_r}{p} \tag{II.26}$$

On the other hand :

$$\omega_r = \frac{d\theta_r}{dt} \tag{II.27}$$

II.5 Park-based transformation:

In order to obtain a mathematical model that is simpler than the physical model of the system, orthogonal transformations are used. In which simple equations by appropriate changes of variables are obtained. Among the most used transformations is that of Park [29].

Park's transformation consists in transforming the system of three-phase stator windings with axes a, b, c, into a system equivalent to two two-phase windings with axes d, q creating the same magneto motive force

The homopolar component does not participate in this creation of fate as the homopolar axis can be chosen orthogonal to the plane (d, q) [29].

II.5.1 Park's matrix in general:

For star 1 is defined as follows:

$$\left[P(\theta_{s1})\right] = \sqrt{\frac{2}{3}}\begin{bmatrix} \cos(\theta) & \cos\left(\theta - \frac{2}{3}\right) & \cos\left(\theta + \frac{2}{3}\right) \\ -\sin(\theta) & -\sin\left(\theta - \frac{2}{3}\right) & -\sin\left(\theta + \frac{2}{3}\right) \\ \frac{1}{\sqrt{2}} & \frac{1}{\sqrt{2}} & \frac{1}{\sqrt{2}} \end{bmatrix} \tag{II.28}$$

$$[P(\theta_{s1})]^{-1} = \sqrt{\frac{2}{3}}\begin{bmatrix} \cos(\theta) & -\sin(\theta) & \frac{1}{\sqrt{2}} \\ \cos\left(\theta-\frac{2}{3}\right) & -\sin\left(\theta-\frac{2}{3}\right) & \frac{1}{\sqrt{2}} \\ \cos\left(\theta+\frac{2}{3}\right) & -\sin\left(\theta+\frac{2}{3}\right) & \frac{1}{\sqrt{2}} \end{bmatrix} \quad \text{(II.29)}$$

• For star 2 and the rotor, we replace in (II.28) et (II.29) θ by $(\theta-\alpha)$ and then by $(\theta_{gl} = \theta - \theta_r)$ respectively.

II.6 Choice of benchmark:

Three types of frames of reference are interesting in practice, the choice of the frame of reference made according to the problem to be studied [30].

II.6.1 Frame of reference linked to the stator ($\omega coor$=0).

$$\frac{d\theta_s}{dt} = 0 \quad \text{(II.30)}$$

$$\theta_s = \theta_r + \theta \quad \text{(II.31)}$$

$$\frac{d\theta_s}{dt} = 0 = \frac{d\theta_r}{dt} + \frac{d\theta}{dt} \quad \text{(II.32)}$$

$$\frac{d\theta_r}{dt} = -\frac{d\theta}{dt} = -p\Omega \quad \text{(II.33)}$$

This reference frame is stationary with respect to the stator, used for the study of starting and braking of alternating current machines with connection of resistors

II.6.2 Referential related to the rotor (ω_{coor}= ω_r).

$$\frac{d\theta_r}{dt} = 0 \quad \text{(II.34)}$$

$$\frac{d\theta_s}{dt} = \frac{d\theta}{dt} = p\Omega \quad \text{(II.35)}$$

This reference frame is stationary with respect to the rotor, used for the study of transient regimes in asynchronous and synchronous machines.

II.6.3 Referential to the rotating field $\omega_s = \omega_e$ et $\omega_r = \omega_e - \omega$

$$\frac{d\theta}{dt} = \omega_s \tag{II.36}$$

$$\frac{d\theta}{dt} = \omega_s - p\Omega \tag{II.37}$$

The latter is used to realize the vector control due to the fact that the manipulated quantities become continuous.

II.7 Park model of the 6PH-IM:

In our work, we used this reference for the modeling of the 6PH-IM. Because this frame of reference is generally used with the aim of being able to apply a command of speed, torque, etc. since the quantities in this frame of reference are continuous. This system of "d, q" axes is fixed with respect to the electromagnetic field created by the stator windings, hence [8].

$\omega_{coor} = \omega_s$

The general expression of the Park transformation is obtained by the projection of the three-phase quantities of the machine on two perpendicular axes d and q.

$$X_{dqo} = P(\theta_s) X_{abc} \tag{II.38}$$

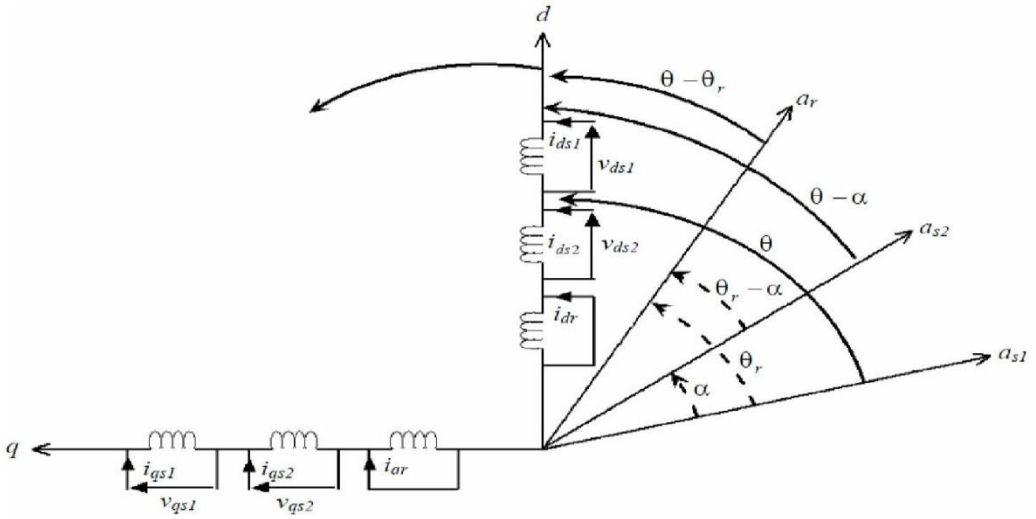

Figure II.2: The generalized model of 6PHIM along the axes

II.7.1 Matrix equation of 6PH-IM with Park transformation

$$\begin{cases} U_{ds1} = R_{s1} i_{ds1} + \dfrac{d}{dt}\varphi_{ds1} - \omega_s \varphi_{qs1} \\ U_{qs1} = R_{s1} i_{qs1} + \dfrac{d}{dt}\varphi_{qs1} + \omega_s \varphi_{ds1} \\ U_{ds2} = R_{s2} i_{ds2} + \dfrac{d}{dt}\varphi_{ds2} - \omega_s \varphi_{qs2} \\ U_{qs2} = R_{s2} i_{qs2} + \dfrac{d}{dt}\varphi_{qs2} + \omega_s \varphi_{ds2} \\ U_{dr} = R_r i_{dr} + \dfrac{d}{dt}\varphi_{dr} - \omega_{gl} \varphi_{qr} \\ U_{qr} = R_r i_{qr} + \dfrac{d}{dt}\varphi_{qr} + \omega_{gl} \varphi_{dr} \end{cases} \quad \text{(II.39)}$$

Or :

$$\omega_{gl} = \omega_s - \omega_r \quad \text{(II.40)}$$

The components of the stator and rotor fluxes are expressed as follows:

$$\begin{cases} \phi_{ds1} = L_{s1} i_{ds1} + L_m \left(i_{ds1} + i_{ds2} + i_{dr} \right) \\ \phi_{qs1} = L_{s1} i_{qs1} + L_m \left(i_{qs1} + i_{qs2} + i_{qr} \right) \\ \phi_{ds2} = L_{s2} i_{ds2} + L_m \left(i_{ds1} + i_{ds2} + i_{dr} \right) \\ \phi_{qs2} = L_{s2} i_{qs2} + L_m \left(i_{qs1} + i_{qs2} + i_{qr} \right) \\ \phi_{dr} = L_r i_{dr} + L_m \left(i_{ds1} + i_{ds2} + i_{dr} \right) \\ \phi_{qr} = L_r i_{qr} + L_m \left(i_{qs1} + i_{qs2} + i_{qr} \right) \end{cases} \quad \text{(II.41)}$$

With :

$$\omega_s = \frac{d\theta}{dt} \quad \text{(II.42)}$$

$$\omega_r = \frac{d\theta_r}{dt} \quad \text{(II.43)}$$

$$p\Omega = \frac{d\theta}{dt} - \frac{d\theta_r}{dt} = \omega_s - \omega_r \quad \text{(II.44)}$$

With :

: Cyclic self-inductance of stator 1. $L_{s1} + L_m$

: Cyclic self-inductance of stator 2. $L_{s2}+L_m$

: Rotor cyclic self-inductance. L_r+L_m

$L_m=\frac{3}{2}L_{ms}=\frac{3}{2}L_{mr}=\frac{3}{2}L_{sr}$: Cyclic mutual inductance between star 1 and 2 and the rotor.

II.8 Put in the form of an equation of state

Putting the system in the form of a state, we find:

$$\left[\dot{I}\right]=[L]^{-1}\left([B][U]-\omega_{gl}[C][I]-[D][I]\right) \quad \text{(II.45)}$$

Or :

$$[B]=diag[1 \quad 1 \quad 1 \quad 1 \quad 0 \quad 0] \quad \text{(II.46)}$$

Command vector:

$$[U]=\left[U_{ds1},U_{qs1},U_{ds2},U_{qs2},U_{dr},U_{qr}\right]^t \quad \text{(II.47)}$$

State vector :

$$[I]=\left[i_{ds1},i_{qs1},i_{ds2},i_{qs2},i_{dr},i_{qr}\right]^t \quad \text{(II.48)}$$

$$\left[\dot{I}\right]=\frac{d}{dt}[I] \quad \text{(II.49)}$$

$$[L]=\begin{bmatrix}(L_{s1}+L_m) & 0 & L_m & 0 & L_m & 0\\ 0 & (L_{s2}+L_m) & 0 & L_m & 0 & L_m\\ L_m & 0 & (L_{s2}+L_m) & 0 & L_m & 0\\ 0 & L_m & 0 & (L_{s2}+L_m) & 0 & L_m\\ L_m & 0 & L_m & 0 & (L_r+L_m) & 0\\ 0 & L_m & 0 & L_m & 0 & (L_r+L_m)\end{bmatrix} \quad \text{(II.50)}$$

$$[C]=\begin{bmatrix}0 & 0 & 0 & 0 & 0 & 0\\ 0 & 0 & 0 & 0 & 0 & 0\\ 0 & 0 & 0 & 0 & 0 & 0\\ 0 & 0 & 0 & 0 & 0 & 0\\ 0 & -L_m & 0 & -L_m & 0 & -(L_r+L_m)\\ L_m & 0 & L_m & 0 & (L_r+L_m) & 0\end{bmatrix} \quad \text{(II.51)}$$

$$[D]=\begin{bmatrix} R_{s1} & -\omega_s(L_{s1}+L_m) & 0 & -\omega_s L_m & 0 & -\omega_s L_m \\ \omega_s(L_{s1}+L_m) & R_{s1} & \omega_s L_m & 0 & \omega_s L_m & 0 \\ 0 & -\omega_s L_m & R_{s2} & -\omega_s(L_{s2}+L_m) & 0 & -\omega_s L_m \\ \omega_s L_m & 0 & -\omega_s(L_{s2}+L_m) & R_{s2} & \omega_s L_m & 0 \\ 0 & 0 & 0 & 0 & R_r & 0 \\ 0 & 0 & 0 & 0 & 0 & R_r \end{bmatrix} \quad \text{(II.52)}$$

II.9 Expressions of the absorbed power and electromagnetic torque

The power of the 6PH-IM in the system of axes (d, q), while neglecting the homopolar components is expressed by:

$$P_a = V_{ds1}i_{ds1} + V_{qs1}i_{qs1} + V_{ds2}i_{ds2} + V_{qs2}i_{qs2} \quad \text{(II.53)}$$

By replacing the voltages $(V_{ds1}, V_{qs1}, V_{ds2}, V_{ds2})$ by their expressions in the equation we find:

$$P_a = \underbrace{\left[R_{s1}i_{ds1}^2 + R_{s1}i_{qs1}^2 + R_{s2}i_{ds2}^2 + R_{s2}i_{qs2}^2\right]}_{Terme\ 1} + \underbrace{\left(\frac{d\varphi_{ds1}}{dt}i_{ds1} + \frac{d\varphi_{qs1}}{dt}i_{qs1} + \frac{d\varphi_{ds2}}{dt}i_{ds2} + \frac{d\varphi_{qs2}}{dt}i_{qs2}\right)}_{Terme\ 2} + \underbrace{\omega_s\left(\varphi_{ds1}i_{qs1} - \varphi_{qs1}i_{ds1} + \varphi_{ds2}i_{qs2} - \varphi_{qs2}i_{ds2}\right)}_{Terme\ 3} \quad \text{(II.54)}$$

This expression is made up of three terms, the first term corresponds to the losses by Joule effect, the second term represents the variation of the electromagnetic energy (energy reserve), the last term is the stored electromagnetic power (Pem).

By the comparison between the universal relation of electromagnetic power and the third term of supplied power:

$$P_{em} = \omega_s\left(\varphi_{ds1}i_{qs1} - \varphi_{qs1}i_{ds1} + \varphi_{ds2}i_{qs2} - \varphi_{qs2}i_{ds2}\right) \quad \text{(II.55)}$$

We find:

$$C_{em} = p\left(\varphi_{ds1}i_{qs1} - \varphi_{qs1}i_{ds1} + \varphi_{ds2}i_{qs2} - \varphi_{qs2}i_{ds2}\right) \quad \text{(II.56)}$$

$$C_{em} = \frac{P_{em}}{\Omega_s} = p\frac{P_{em}}{\omega_s} \quad \text{(II.57)}$$

Other expressions of the electromagnetic torque are possible. By replacing the expressions(II.40) in (II.56), we get :

$$C_{em} = pL_m \{(i_{qs1} + i_{qs2})i_{dr} - (i_{ds1} + i_{ds2})i_{qr}\} \quad \text{(II.58)}$$

From the rotor flux equations (φ_{dr} et φ_{qr}) expressed by (III.40), we get

$$i_{dr} = \frac{1}{L_m + L_r}[\varphi_{dr} - L_m(i_{ds1} + i_{ds2})] \quad \text{(II.59)}$$

$$i_{qr} = \frac{1}{L_m + L_r}[\varphi_{qr} - L_m(i_{qs1} + i_{qs2})] \quad \text{(II.60)}$$

By replacing (III.59) and (III.60) in the equation (III.58), we will have the relation of the electromagnetic torque in the Park frame (d, q) as follows:

$$C_{em} = p\frac{L_m}{L_m + L_r}\{(i_{qs1} + i_{qs2})\varphi_{dr} - (i_{ds1} + i_{ds2})\varphi_{qr}\} \quad \text{(II.61)}$$

II.10 Simulation of the 6PH-IM powered by sinusoidal voltages

The simulation consists of implementing the electromechanical model of 6PH-IM under the Mat lab/Simulink environment[31].

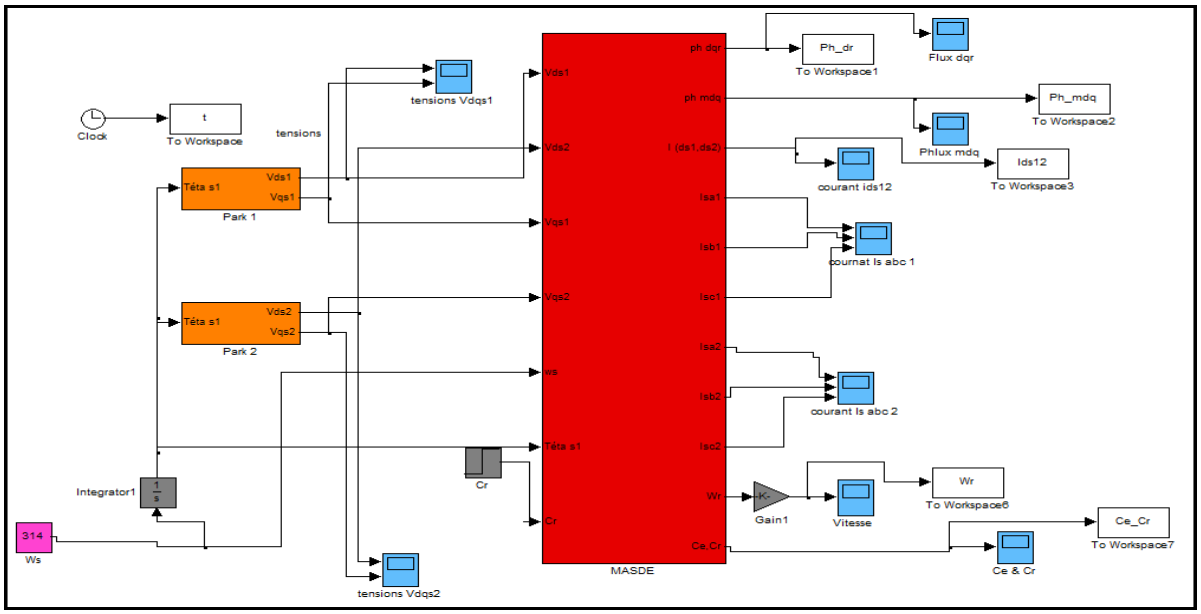

Figure II.3 : The simulation block diagram

II.10.1 Simulation Results:

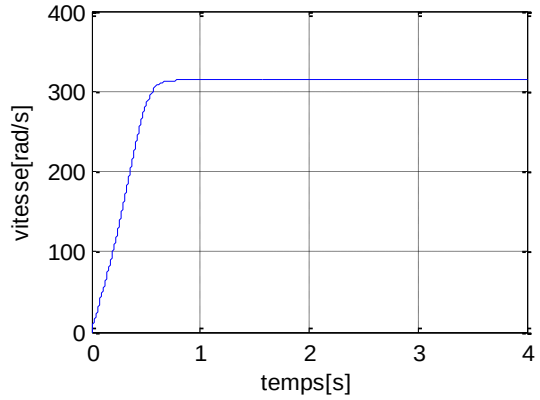

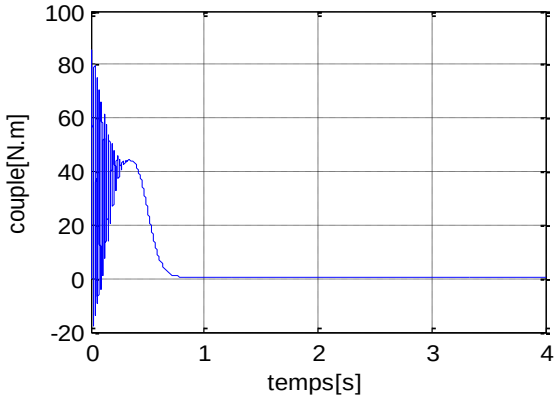

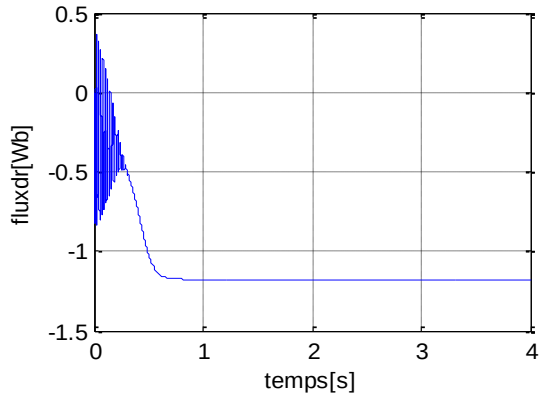

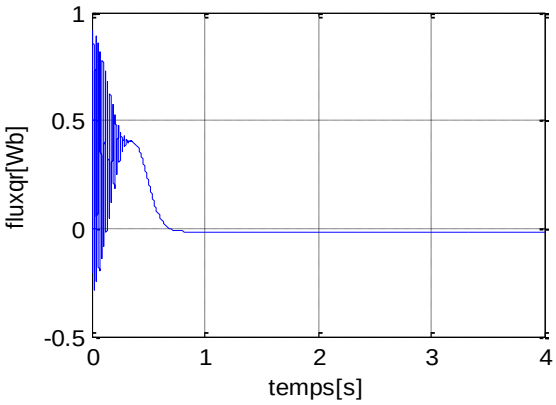

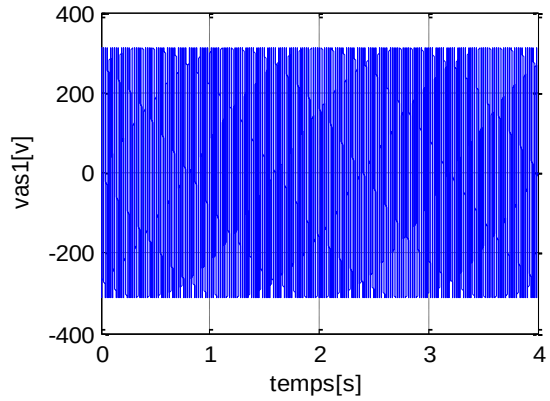

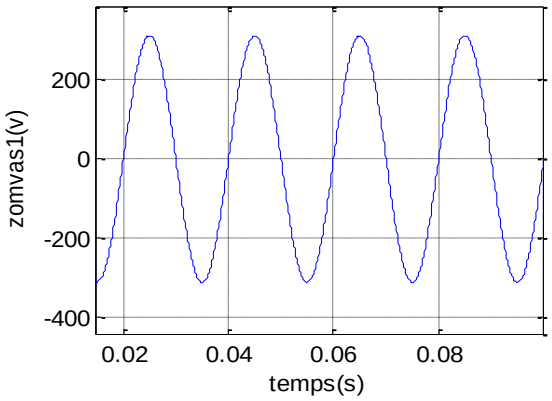

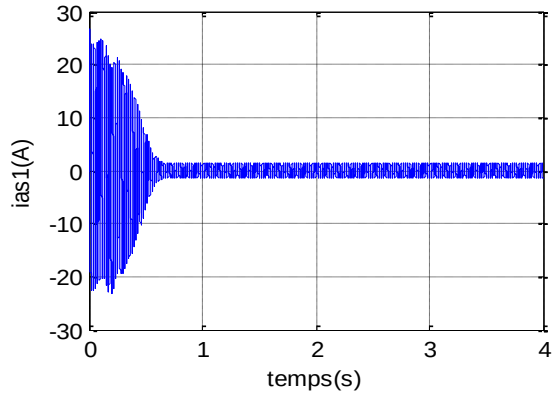

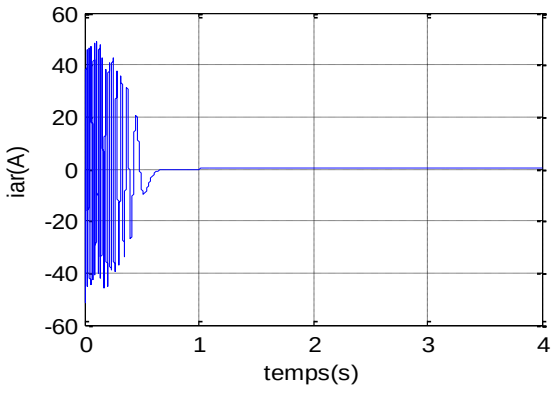

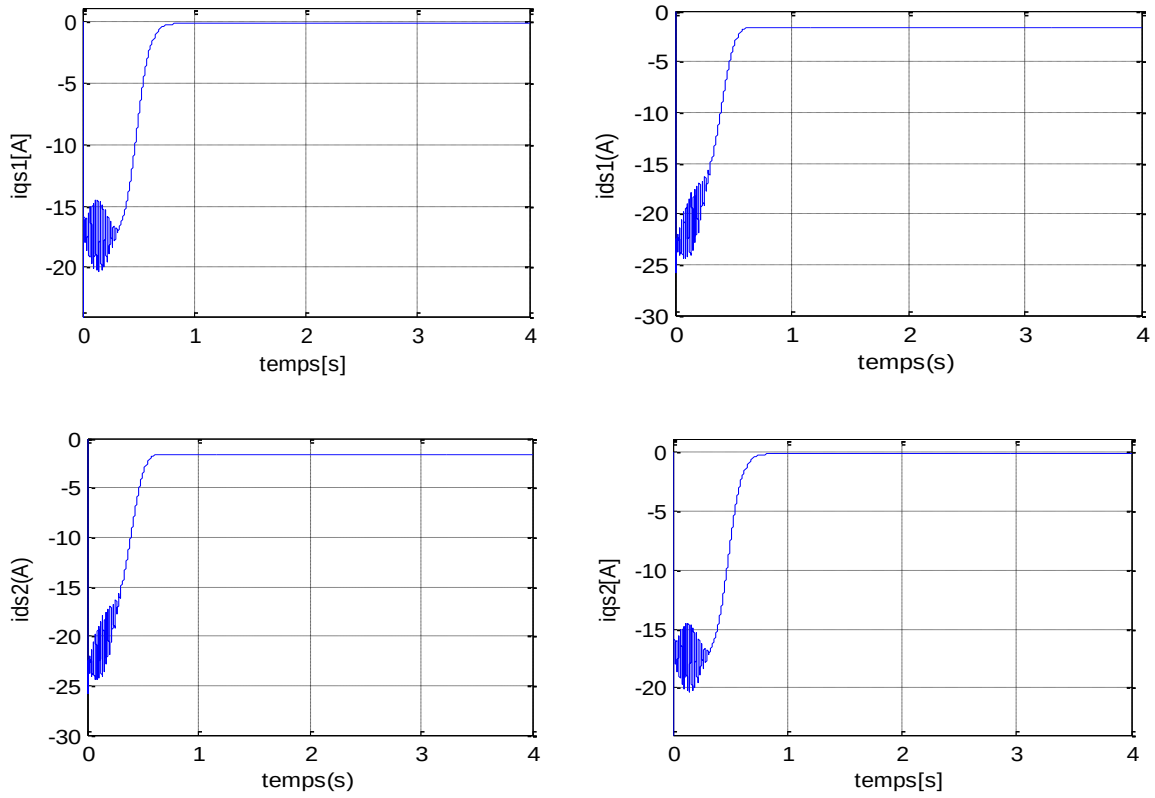

Figure II.4: Performances de la six phase induction machine lors d'un démarrage à vide.

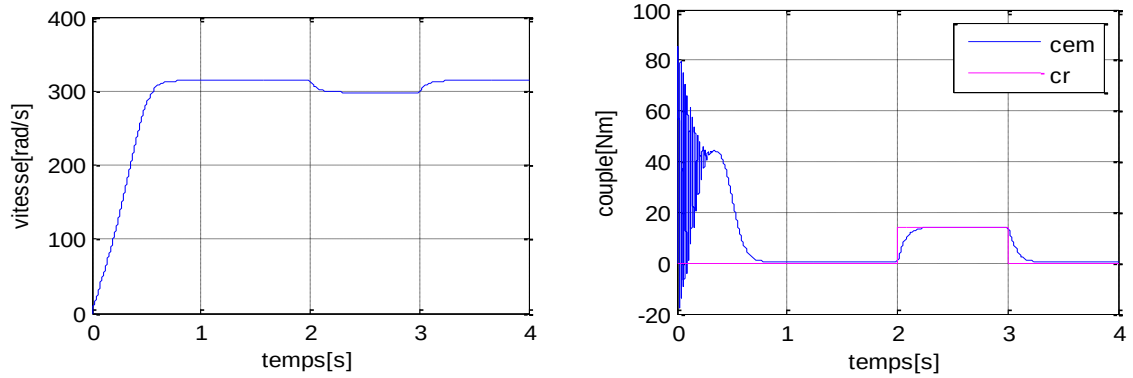

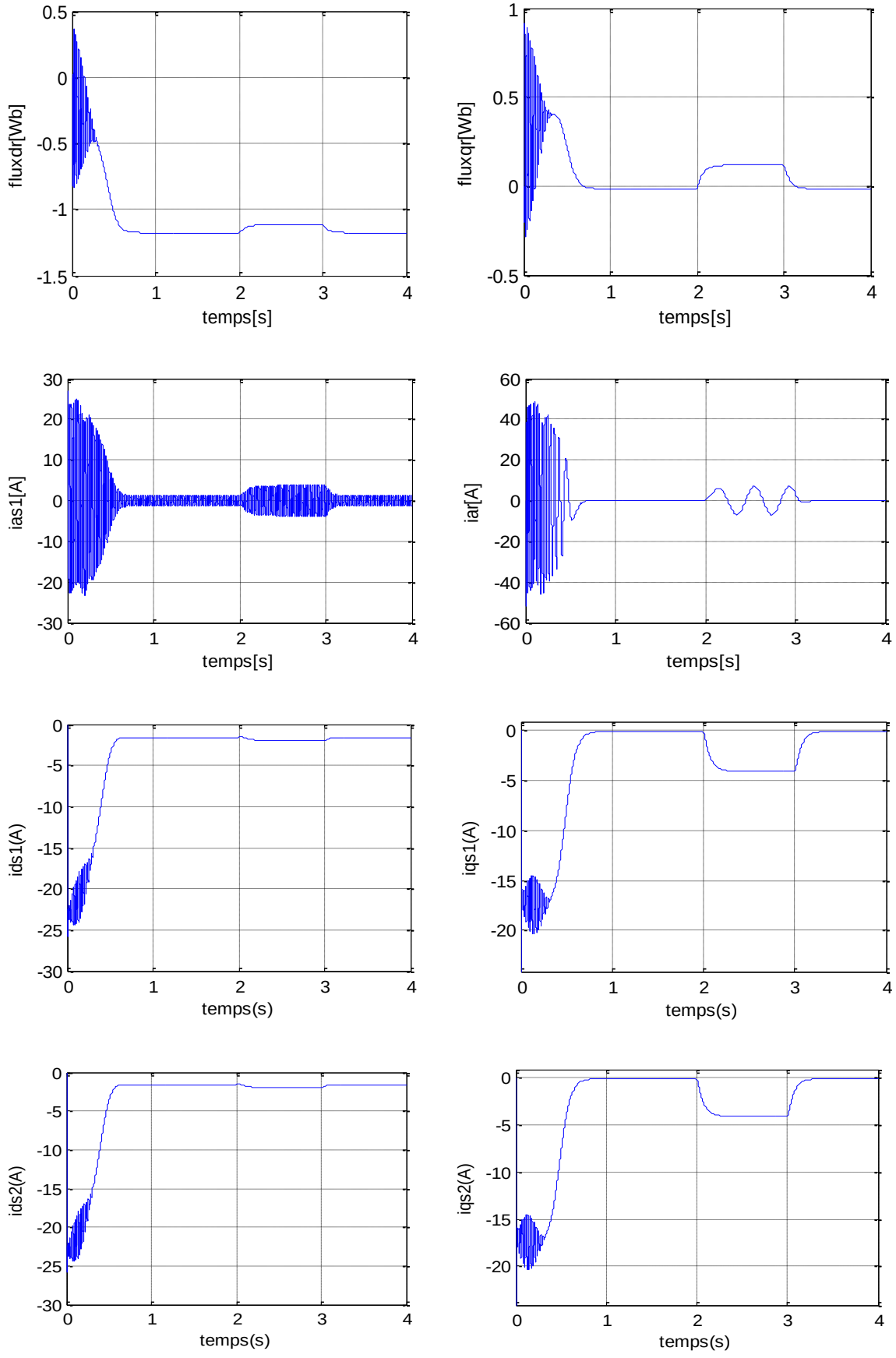

Figure II.5: Performances de la six phase induction machine avec application d'un couple de charges Cr=14 N.m between 2s et 3s

II.10.2 Discussion of the results

We simulated the operation of the asynchronous double stator machine powered directly from the standard network (220/ 380V, 50Hz), empty and loaded.

The simulation results given by the figures (Figure II.5 and Figure II.4), these figures represent the evolution of some fundamental variables of the asynchronous machine, namely the speed of rotation (ω_r), the electromagnetic torque (Cem), stator phase currents (i_{sa1}, i_{sa2}), currents according to axes d and q (i_{sd1} i_{sd2}, i_{sq1} i_{sq2}) and rotor flux (flux rd, flux rq).

At start-up and during the transient speed, the speed increases and evolves in an almost linear manner and reaches 313.8 rad/s à $t \approx 0.8$s (start of permanent diet).

The electromagnetic torque, at the beginning reaches its maximum value of 85.4N.m, and presents oscillations that disappear after 0.4 s, where it reaches 42.4 N.m, then it decreases in an almost linear way and stabilizes at its minimum value of 0.314 N.m, which is due to friction. The stator currents (stars 1 and 2) show excessive exceedances inducing strong current calls of about 4 times the nominal current, but which disappears after some alternations to give rise to sine forms of constant amplitude. The stator currents along the direct and quadrature axes evolve in a manner roughly analogous to the evolution of the velocity; nevertheless, there are slight oscillations at the level of the latter during approximately 0.3s. The evolution of rotor flows is almost identical to that of the electromagnetic couple.

Applying a strong torque load, Cr = 14 N.m (engine-running machine) from the moment t = [2,3]s, we see that the speed and currents according to (d,q) decrease and stabilize respectively at w_r= 298 rad/s , $i_{ds1} = i_{ds2} = -1.97$A et $i_{qs1} = i_{qs2} = -4.13$A; in contrast, increases are observed in the electromagnetic torque, stator currents (stars 1 and 2) and at the rotor flow level according to (d,q), which stabilize respectively at Cem = 14.33 N.m (slightly more than the load torque), $i_{as1} = i_{as2} = 3.74$A, flux dr = −1.11wb et flux qr = 0.11wb.

However, in motor operation, the slippage of the machine becomes a little more important than at vacuum, the supply voltage V_{as1} and stator current $i_{as1}$are almost in phase and of the same sign; however, the offset behind the current in relation to the voltage due to the inductive effect of the machine, the two quantities are of the same sign means that the direction of transition of the power is positive.

II.11 Conclusion :

In this chapter, we studied the modeling of 6PH-IM machine as motor. This modeling allowed us to establish a mathematical model of this machine whose complexity was reduced by numbers of simplifying hypotheses. Thus, we applied Park's transformation to the equations of system in order to facilitate their implementation through Matlab Simulink. Then we interpreted the obtained results.

The insertion of the load causes a variation in speed and shows the strong coupling that exists between the two axes (d q) which makes separate control very difficult. To solve this problem, we propose in the next chapter the vector control technique which based on the flux orientation which allows a decoupling of the system and facilitates the independent adjustment of each axis.

CHAPTER III

Field oriented control of the 6PH-IM powered by two-level converters

III.1 Introduction

Vector control was initially introduced by Blascke in 1972 . However, it could only be implemented and used with advances in microelectronics. Indeed, it requires Park transform calculations, evaluation of trigonometric functions, integrations, regulations etc., which could not be done in pure analog.

In this chapter, we will apply vector control by orientation of the rotor flux on the 6PH-IM. However, we first present a reminder of the principle and the different methods of vector control, we then give the application of the latter on the MASDE, and we will finally comment on the provided performance by this type of adjustment after the obtaining and illustrating simulation results.

III.2 Modelling of the machine feed.

In the supply of the variable frequency machine the static converter is used, which delivers, controls the frequency and amplitude of the stator voltages or the amplitude of the stator currents. The frequency is proportional to the speed of the machine. In this study, the static converter consists of three stages:

A rectifier connected to the three-phase power supply network, which transforms the AC voltage into a continuous, LC low-pass filter that reduces current and voltage ripples, and for the existence of the two stator windings require two inverters controlled by MLI which allow to supply the machine by a system of alternating voltage with variable frequency. The general structure of feeding is given in figure (III.1).

The required characteristics of the electric actuator depend on the machine, the power supply of the network and the type of control applied to the frequency converter. Thèse characteristics are [32] :

- A torque with the minimum possible ripple, controllable by the smallest number of variables, in both dynamic and steady state.
- A wide range of speed variation.
- Low electrical and mechanical time constants.
- The three-phase power source is assumed to be symmetric, frequency and constant amplitude

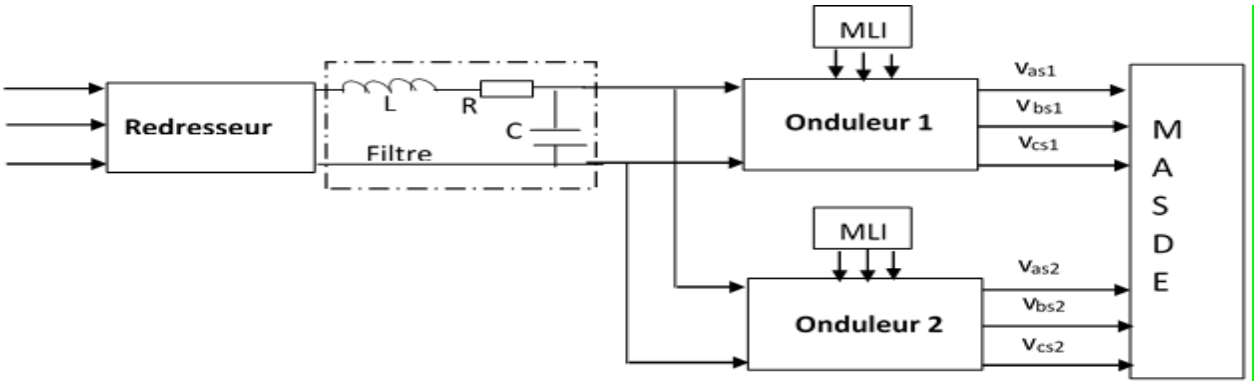

Figure III.1: synoptic diagram of a 6PH-IM and its power supply.

III.2.1 Rectifier Modeling:

Diode and thyristor rectifiers provide continuous alternative conversion, fed from the single-phase or three-phase network, they provide the output with a continuous voltage of fixed or variable value, either for direct feeding to a receiver, or to power another converter. [33]

In our work, we are only interested in the 3-phase, uncontrolled dual-alternation rectifier with diode components (Figure III.2). Rectifier power is supplied through the three-phase power grid where the voltage system is balanced.

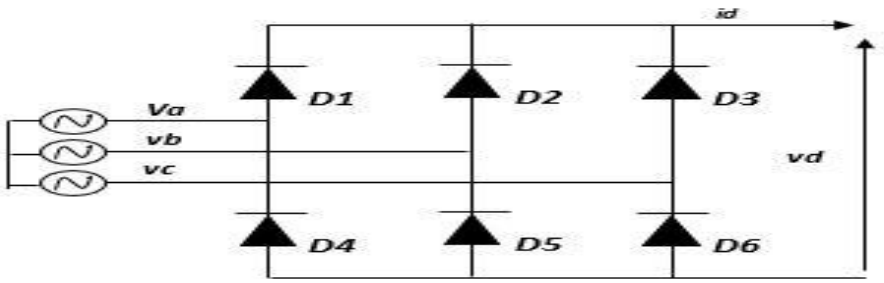

Figure III.2: Representation of the three-phase diode

This rectifier has three diodes (D_1, D_2, D_3) with common cathode providing current and three diodes (D_4, D_5, D_6) common anode ensuring current return.

The rectifier is powered by a balanced three-phase system with constant voltage and frequency amplitude. Voltage drops and losses in the diodes are ignored. The rectifier is then powered by the following three-phase system:

$$U_a(t) = V_m \sin(wt) \quad \text{(III.1)}$$

$$U_b(t) = V_m \sin\left(wt - \frac{2\pi}{3}\right) \quad \text{(III.2)}$$

$$U_c(t) = V_m \sin(wt - \frac{4\pi}{3}) \quad \text{(III3.)}$$

The voltage at the rectifier output is given by :

$$U_{red}(t) = Max[U_a(t), U_b(t), U_c(t)] - Min[U_a(t), U_b(t), U_c(t)] \quad \text{(III.4)}$$

And its average value is given by :

$$U_{d\,moy} = \frac{3\sqrt{3}.\ V_m}{\pi} \quad \text{(III.5)}$$

Its ripple factor is given by:

$$K\% = \frac{U_{d\,max} - U_{d\,min}}{2.U_{d\,moy}} = 7\% \quad \text{(III.6)}$$

The diagram in Figure III.3 shows the speed of the three-phase voltage system (U_a, U_b, U_c) *at the rectifier bridge inlet and the straightened voltage* U_d at the exit of this one.

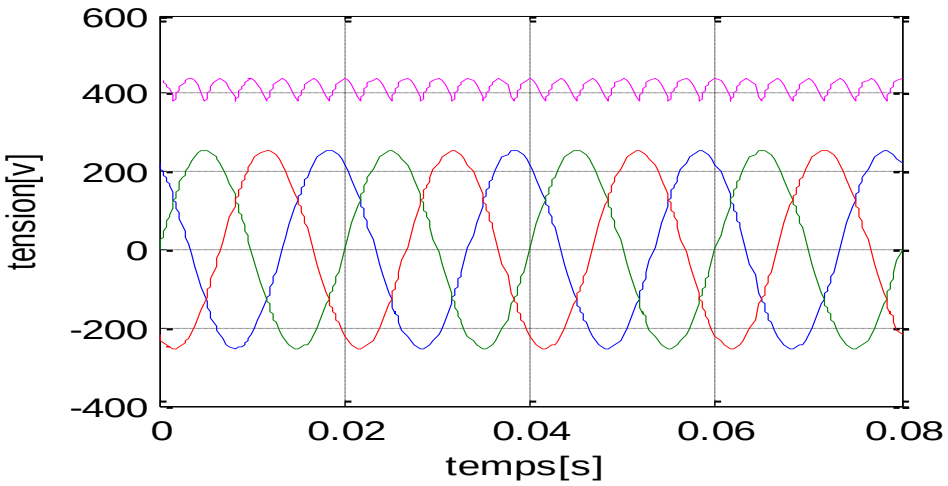

Figure III.3: Supply voltages and rectified voltage.

The voltage obtained by this rectifier has significant ripples, which requires a filter to decrease these ripples.

III.2.2 Filter modeling:

Between the rectifier bridge and the two voltage inverters, a LC filter is inserted (passebas) to decrease the ripples of the voltage source and continuous current as shown in figure(III.4).

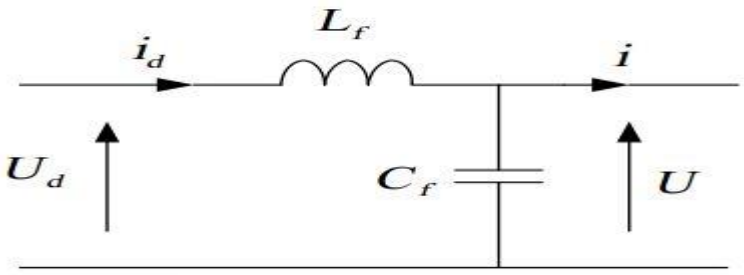

Figure III.4: Filter diagram.

- Capacity C_f allows to obtain at the input of the inverter a substantially constant voltage U, and to absorb the negative current returned by the load.
- inductance L_f can reduce current ripples i_d.

This filter is modeled by the following equations:

$$\begin{cases} U_d = L_f \frac{di_d}{dt} + U \\ \frac{dU}{dt} = \frac{1}{C_f}(i_d - \mathrm{I}) \end{cases} \quad \text{(III.7)}$$

The filter transfer function is given by the following relation :

$$F(s) = \frac{U(s)}{U_d(\mathrm{s})} = \frac{1}{L_f C_f s^2 + 1} \quad \text{(III.8)}$$

This is a second order function, the cut frequency is:

$$f_c = \frac{1}{\sqrt{L_f . C_f}} \quad \text{(III.9)}$$

To size the filter, the choice of values of inductance and capacity can be obtained by laying down the simple condition that consists in eliminating harmonics of order greater than or equal to two. Resonant pulse is significantly higher than the use pulse.

III.3 Modeling of the two level inverters

A stand-alone inverter (with PWM control) is a static converter which ensures the transformation of the energy of a continuous source into an alternative energy, which can be at fixed or variable frequency

The speed and torque control of the 6PH-IM is carried out by simultaneous action on the frequency and on the amplitude of the stator voltage, based on variable frequency voltage inverters. Each 6PH-IM star is connected to a three-phase inverter with controlled switching. The latter consists of three branches where each is composed of two pairs of supposedly perfect switches and whose commands are disjoint and complementary;

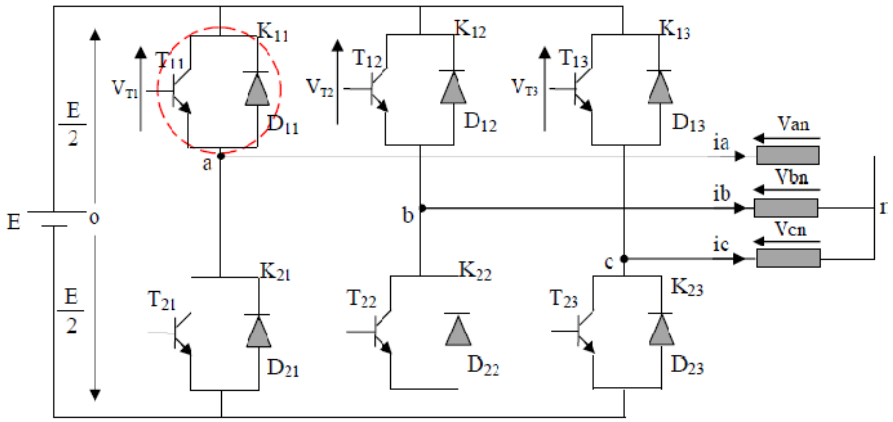

Figure III.5: Scheme Two-level three-phase voltage inverter.

Each switch (transistor + diode) (Figure III.5), (, i = 1, 2 or 3 j = 1 or 2), supposedly idealized. We can establish the relations:

$$V_{10} - V_a + V_b - V_{20} = 0 \qquad \text{(III.10)}$$

$$V_{10} - V_a + V_c - V_{30} = 0 \qquad \text{(III.11)}$$

Adding these equations, we get:

$$2V_{10} - 2V_a + V_b + V_c - V_{20} - V_{30} = 0 \qquad \text{(III.12)}$$

The single voltages form a balanced three-phase system such as:

$$V_a + V_b + V_c = 0 \tag{III.13}$$

In(III.12), we can replace by and we get

$$\begin{cases} V_a = \frac{1}{3}(2V_{10} - V_{20} - V_{30}) \\ V_b = \frac{1}{3}(-V_{10} + 2V_{20} - V_{30}) \\ V_c = \frac{1}{3}(-V_{10} - V_{20} + 2V_{30}) \end{cases} \tag{III.14}$$

each switch is represented by a transistor-diode pair which is modeled by two states defined by the following logic connection function:

$$f_i = \begin{cases} 1 \quad l'\text{int } \textit{érrupteur} \quad i \quad est \quad fermé \quad (K_i \quad conduit, \quad \overline{K_i} \quad bloqué) \\ 0 \quad l'\text{int } \textit{érrupteur} \quad i \quad est \quad ouvert \quad (K_i \quad bloqué, \quad \overline{K_i} \quad conduit) \end{cases}$$

With:

$$f_i + \overline{f_i} = 1 \quad et \quad i = 1...3.$$

The equation in matrix form we have:

$$\begin{bmatrix} V_a \\ V_b \\ V_c \end{bmatrix} = \frac{E}{3}\begin{bmatrix} 2 & -1 & -1 \\ -1 & 2 & -1 \\ -1 & -1 & 2 \end{bmatrix}\begin{bmatrix} f_{11} \\ f_{21} \\ f_{31} \end{bmatrix} \tag{III.15}$$

III.4 Inverter control strategy

The control of the inverter by PWM (Pulse Width Modulation) makes it possible to produce from a source at fixed frequency and voltage, alternating voltages variable in amplitude and frequency, with a low harmonic content. For our study we apply the sine-triangle PWM control strategy [34].

III.4.1 Control by sine-delta modulation

The sine-triangle PWM is produced by comparing a low-frequency modulating wave (reference voltage) to a triangular-shaped high-frequency carrier wave.

The instants of switching are determined by the points of intersection between the carrier and the modulating. The switching frequency of the switches is fixed by the carrier [34].

The sinusoidal reference voltages are expressed by:

For the first star:

$$\begin{cases} V_{refa1} = V_m \sin(2\pi ft) \\ V_{refb1} = V_m \sin(2\pi ft - \frac{2}{3}) \\ V_{refc1} = V_m \sin(2\pi ft + \frac{2}{3}) \end{cases} \quad \text{(III.16)}$$

For the second star; It suffices to replace in the system of equations , by and the index 1 by 2.

$$V_p(t) = \begin{cases} V_{pm}\left[4(t/T_p) - 1\right] & Si \quad 0 \le t \le T_p/2 \\ V_{pm}\left[-4(t/T_p) + 3\right] & Si \quad T_p/2 \le t \le T_p \end{cases} \quad \text{(III.17)}$$

This technique is characterized by the following two parameters:

- The modulation index m_{mod} equal to the ratio of the modulation frequency(f_p) on the reference frequency (f);
- The voltage adjustment coefficient r equal to the ratio of the amplitude of the reference voltage (V_m) at the peak value of the modulation wave (V_{pm})

III.5 Association of the 6PH-IM with static voltage converters controlled by PWM control

The schematic representation of the association of the 6PH-IM with two voltage inverters with sine-delta PWM control is given by the figure III.6

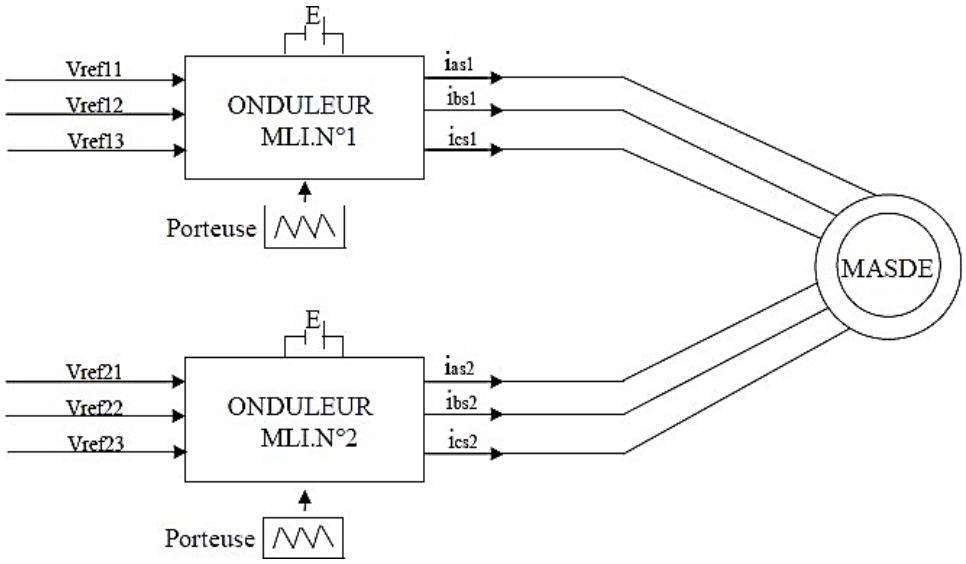

Figure III.6 : Association of the 6PH-IM static voltage converters with PWM control

III.6 Origins of Vector Control :

The origins of vector control, contrary to popular belief, go back to the end of the XIXth century and to the works of A. Blondel on the theory of the reaction of the two axes. However, given the technology used at that time, there was no question to transfer this theory to the control of electrical machines. It is only towards end of the fifties thanks to the use in Eastern Europe of the method of [35].

III.7 Principle of Vector Control :

The principle of vector control (or oriented flux control) consists in directing one of the stator, rotor or air gap flux components on an axis of the reference frame rotating at the speed ωs.

The purpose of this command is to assimilate the behavior of the six-phase induction machine to that of a DC machine with separate excitation figure (III.7).

Indeed in a DC machine the armature current Ia controls the torque and the field current If controls the flux [36].

The expression of the electromagnetic torque of the MCC is given by:

$C_{em} = K\Phi I_a = K' I_a I_f.$

With:

Φ : Flux imposed by the excitation currentIf.

Ia: Armature current.

K, K': Constants.

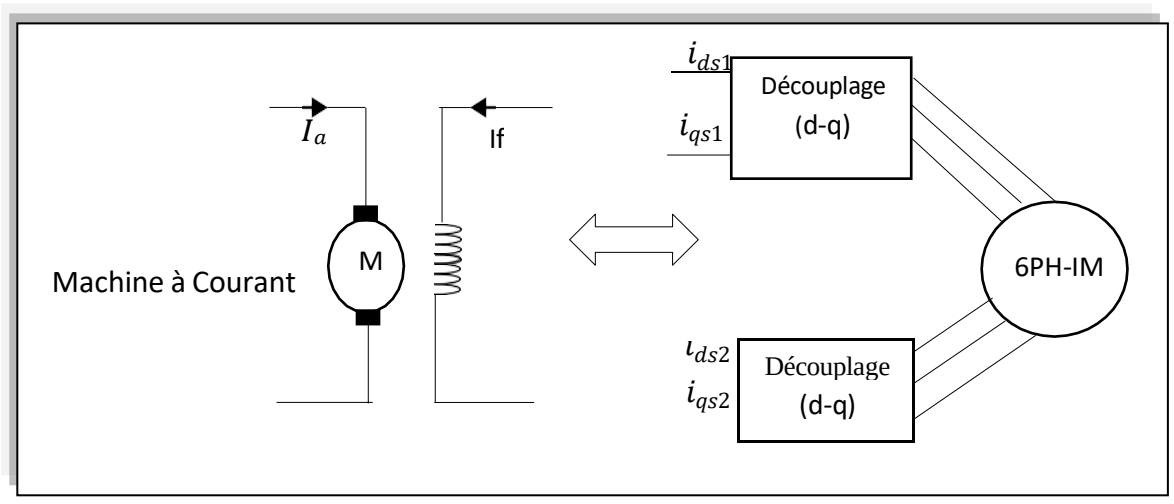

Figure III.7: The principle of vector control

In the expression of the electromagnetic torque of 6PH-IM, if we apply the orientation condition.

$$C_{em} = p\frac{L_m}{L_m+L_r}[(i_{qs1} + i_{qs2})\emptyset_{dr} - (i_{ds1} + i_{ds2})\emptyset_{qr}] \quad \text{(III.18)}$$

The equation then becomes:

$$C_{em} = p\frac{L_m}{L_m+L_r}[(i_{qs1} + i_{qs2})\emptyset_r] = K''\emptyset_r i_q \quad \text{(III.19)}$$

III.8 Flux orientation process

There are three types of Flux orientation

Orientation of the rotor flux with the conditions $\emptyset_{dr} = \emptyset_r \emptyset_{qr} = 0$

Orientation of the stator flux with the conditions $\emptyset_{ds} = \emptyset_s \emptyset_{qs} = 0$

Air gap Flux direction with conditions $\emptyset_{dm} = \emptyset_m \ \emptyset_{qm} = 0$

Many researchers use the orientation of the rotor flux for the control of the electric machine . In our study, we opted for the technique

orientation of the rotor flux. For the six-phase induction machine, vector control consists in decoupling the quantities generating the electromagnetic torque and the rotor flux. In the expression of the electromagnetic torque of the 6PH-IM, (3.2), if one coincides the rotor flux with the axis (d) of the reference frame related to the field

turning, that is to say: : $\emptyset_{dr} = \emptyset_r \quad \emptyset_{qr} = 0$.

$$C_{em} = p\frac{L_m}{L_m+L_r}[(i_{qs1} + i_{qs2})\emptyset_{dr} - (i_{ds1} + i_{ds2})\emptyset_{qr}] \quad \text{(III.20)}$$

The equation then becomes:

$$C_{em} = p\frac{L_m}{L_m+L_r}[(i_{qs1} + i_{qs2})\emptyset_r] = K''\emptyset_r i_q \quad \text{(III.21)}$$

From equation (IV.3) we find that the electromagnetic torque results from the interaction of a flux term and a current term. This expression refers to the torque of the separately excited DC machine. It is therefore concluded that the operation of the six-phase induction machine, with its vector control, is similar to that of the DC machine with separate excitation[37].

III.9 Vector Control Methods

The vector control technique of the 6PH-IM can be either direct or indirect [38].

III.9.1 Direct control Method

This method consists in determining the position and the modulus of the flux whatever the operating regime. Two methods are used for this:

- Measuring the flux in the air gap of the machine using a sensor, the main drawback of this technique lies in the fact that the flux sensors are mechanically very fragile.
- Flux estimation using mathematical methods. This method is sensitive to variations in machine parameters

III.9.2 Indirect control method

This method does not use the amplitude of the rotor flux but only its position, it does not require the use of a rotor flux sensor but requires the use of a position (speed) sensor or estimator rotor**.**

The major drawback of this method is the sensitivity of the estimate towards the variation of the machine parameters due to the magnetic saturation and the variation of the temperature, especially the rotor time constant.

III.10 Speed control by the direct method:

Direct vector control requires knowledge of the module and the position of the rotor flux. For this purpose, an estimator of the rotor flux φr is implemented from the measurements of stator currents and the transformed into $ids1$, $iqs1$, $ids2$ $etiqs2$ and the slip pulsation [39]. The figure (III.8) represents the simplified block diagram of the flux-orientedcontrol.

Figure III.8: Simplified block diagram of flux oriented control (FOC)

By applying the orientation of the rotor flux to the system equations (II.61) becomes:

$$I_{dr} = \frac{1}{L_m+L_r}[\emptyset_r - L_m(i_{ds1} + i_{ds2})] \quad \text{(III.22)}$$

$$I_{qr} = \frac{-L_m}{L_m+L_r}(i_{qs1} + i_{qs2}) \quad \text{(III.23)}$$

Substituting (2.3) and (2.4) in (I.42) we find

$$\begin{aligned} \emptyset_{ds1} &= \lambda_1 i_{ds1} + L_r \eta i_{ds2} + \eta \emptyset_r^* \\ \emptyset_{qs1} &= \lambda_1 i_{qs1} + L_r \eta i_{qs2} \\ \emptyset_{ds2} &= \lambda_2 i_{ds2} + L_r \eta i_{ds1} + \eta \emptyset_r^* \\ \emptyset_{qs2} &= \lambda_2 i_{qs2} + L_r \eta i_{qs1} \end{aligned} \quad \text{(III.24)}$$

With:

$$\eta = \frac{L_m}{L_m+L_r} \; ; \; \lambda_{1,2} = L_{s1,s2} + \eta L_r \quad \text{(III.25)}$$

And we have :

$$\emptyset_r^* = L_m(i_{ds1} + i_{ds2}) \quad \text{(III.26)}$$

$$I_{qr} = \frac{-\omega_{gl}\emptyset_r^*}{R_r} \quad \text{(III.27)}$$

By replacing in the system of stator voltage equations (II.39), we obtain:

$$\begin{aligned} v_{ds1}^* &= R_{s1} i_{ds1} + L_{s1}\frac{d}{dt} i_{ds1} - \omega_s^*(L_{s1} i_{qs1} + T_r \emptyset_r^* \omega_{gl}^*) \\ v_{qs1}^* &= R_{s1} i_{qs1} + L_{s1}\frac{d}{dt} i_{qs1} - \omega_s^*(L_{s1} i_{ds1} + \emptyset_r^*) \\ v_{ds2}^* &= R_{s2} i_{ds2} + L_{s2}\frac{d}{dt} i_{ds2} - \omega_s^*(L_{s2} i_{qs2} + T_r \emptyset_r^* \omega_{gl}^*) \\ v_{qs2}^* &= R_{s1} i_{qs2} + L_{s2}\frac{d}{dt} i_{qs2} - \omega_s^*(L_{s2} i_{ds2} + \emptyset_r^*) \end{aligned} \quad \text{(III.28)}$$

Sur un:

$$i_{qs1}^* + i_{qs2}^* = \frac{(L_m+L_r)}{pL_m\emptyset_r^*} C_{em}^* \quad \text{(III.29)}$$

$$\omega_{gl}^* = \frac{R_r L_m}{(L_m+L_r)\emptyset_r^*}(i_{qs1}^* + i_{qs2}^*) \quad \text{(III.30)}$$

The torque expression shows that the reference flux and the quadrature stator currents are not perfectly independent. For this, it is necessary to decouple the torque control and the flux control of this machine by introducing new variables:

$$v_{ds1l} = R_{s1} i_{ds1} + L_{s1} \frac{d}{dt} i_{ds1}$$
$$v_{qs1l} = R_{s1} i_{qs1} + L_{s1} \frac{d}{dt} i_{qs1} \quad \text{(III.31)}$$
$$v_{ds2l} = R_{s2} i_{ds2} + L_{s2} \frac{d}{dt} i_{ds2}$$
$$v_{qs2} = R_{s2} i_{qs2} + L_{s2} \frac{d}{dt} i_{qs2}$$

The system (III.15) implies that the stator voltages and currents are directly related. To compensate for the error introduced during decoupling, the reference stator voltages are introduced:

$$v_{ds1}^{*} = v_{ds1l} - v_{ds1c}$$
$$v_{qs1}^{*} = v_{qs1l} + v_{qs1c}$$
$$v_{ds2}^{*} = v_{ds2l} - v_{ds2c} \quad \text{(III.32)}$$
$$v_{qs2}^{*} = v_{qs2l} + v_{qs2c}$$

With:

$$v_{ds1c} = \omega_s^{*}(L_{s1} i_{qs1} + T_r \emptyset_r^{*} \omega_{gl}^{*})$$
$$v_{qs1c} = \omega_s^{*}(L_{s1} i_{ds1} + \emptyset_r^{*})$$
$$v_{ds2c} = \omega_s^{*}(L_{s2} i_{qs2} + T_r \emptyset_r^{*} \omega_{gl}^{*}) \quad \text{(III.33)}$$
$$v_{qs2c} = \omega_s^{*}(L_{s2} i_{ds2} + \emptyset_r^{*})$$

For a perfect decoupling, we add the regulation loops of the stator currents $i$ds1, $i$ds1, $i$qs1, $i$qs2 we obtain at their outputs the stator voltages, .V_{ds1}, V_{ds2}, V_{qs1}, V_{qs2}.

III.11 Synthesis of PI controllers

The purpose of using controllers is to ensure better robustness against internal or external disturbances[40].

The identification of the parameters of the PI controllers of the systems whose transfer function is of the first order, such as :

$$H(s) = \frac{1}{\mathrm{as+b}} \quad \text{(III.34)}$$

Generally done as follows:

The transfer function of a PI regulator is:

$$C(s) = K_p + \frac{K_i}{S} \quad \text{(III.35)}$$

With:

Kp: the proportionality coefficient;

Ki: the coefficient of integration;

The representative diagram of the regulation loop of a first order servo system with unit feedback regulated by a PI is given by the figure

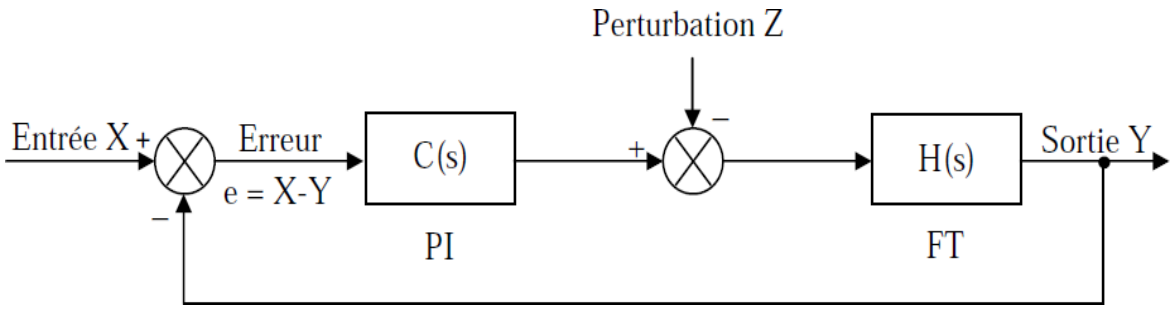

Figure III.09: First-order servo system controlled by a PI.

The disturbance is generally neglected in the steps of identifying the parameters of the controllers.

The open loop transfer function of the servo system is:

$$T(s) = C(s)H(s) = \frac{K_p S + K_i}{aS^2 + bS} \quad \text{(III.36)}$$

In closed loop we get:

$$F(s) = \frac{T(s)}{1+T(s)} = \frac{K_p S + K_i}{aS^2 + (K_p + b)S + K_i} \quad \text{(III.37)}$$

In control to have a behavior of a first control system whose transfer function is of the form:

$$G(s) = \frac{1}{rs+1} \quad \text{(III.38)}$$

It suffices to identify (II.23) with (II.24) as follows:

$$\frac{K_p S + K_i}{aS^2 + (K_i + b)S + K_i} = \frac{1}{rs+1} \quad \text{(III.39)}$$

Which give:

$$aS^2 + (K_P + b)S + K_i = K_P\tau S^2 + (K_P + K_i\tau)S + K_i \quad \text{(III.40)}$$

$$K_p = \frac{a}{\tau} \quad \text{(III.41)}$$

$$K_i = \frac{b}{\tau} \quad \text{(III.42)}$$

III.11.1 Parameters of current PI controllers:

Figure (III.10) shows the diagram of the stator current regulation loop (stars 1 and 2).

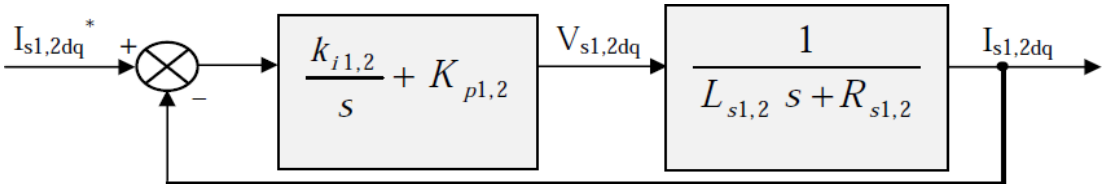

Figure III.10 : Stator current regulation loop.

With:

$$\mathbf{K_{P1}} = \frac{L_{s1}}{r} \quad \text{et} \quad \mathbf{K_{P2}} = \frac{L_{s2}}{r} \quad \text{(III.43)}$$

$$\mathbf{K_{i1}} = \frac{R_{s1}}{r} \qquad \mathbf{K_{i2}} = \frac{R_{s2}}{r}$$

We take $r = r_r/6$ to have fast process dynamics, with $rr = Lr/Rr$ being the electrical (rotor) time constant of the system.

The voltage decoupling block diagram (Field Oriented Control: FOC) is shown in Figure (III.11).

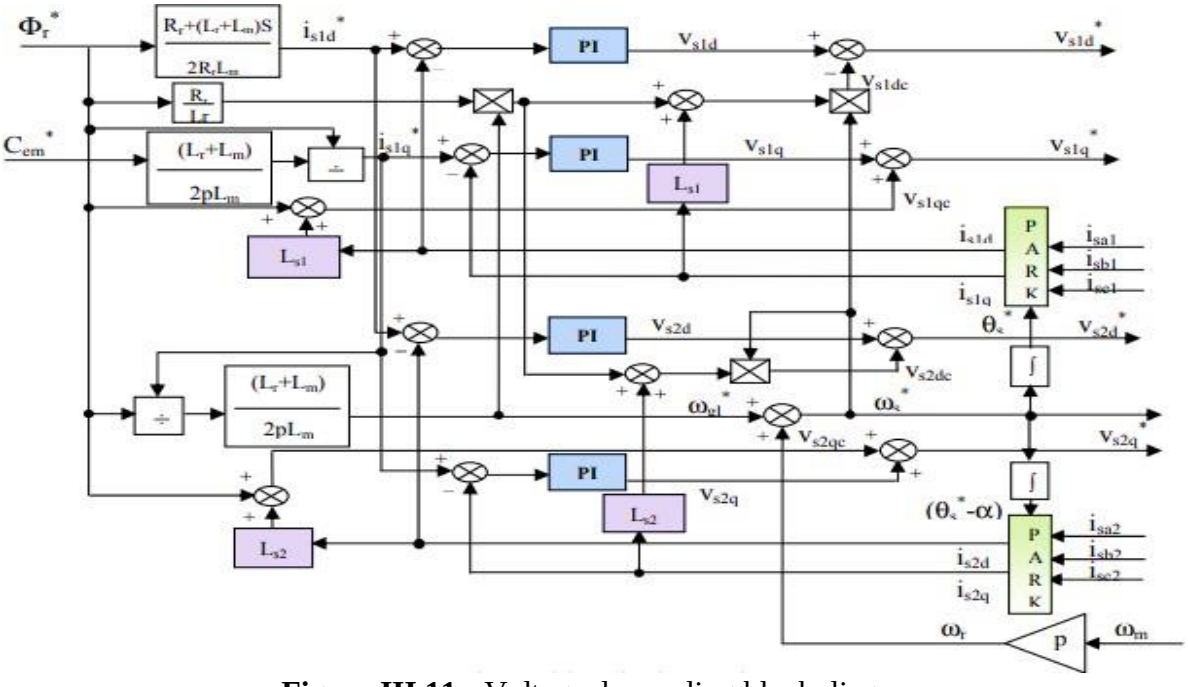

Figure III.11 : Voltage decoupling block diagram

III.11.2 The parameters of the speed PI controllers:

The speed regulation diagram is given by the following figure III.12:

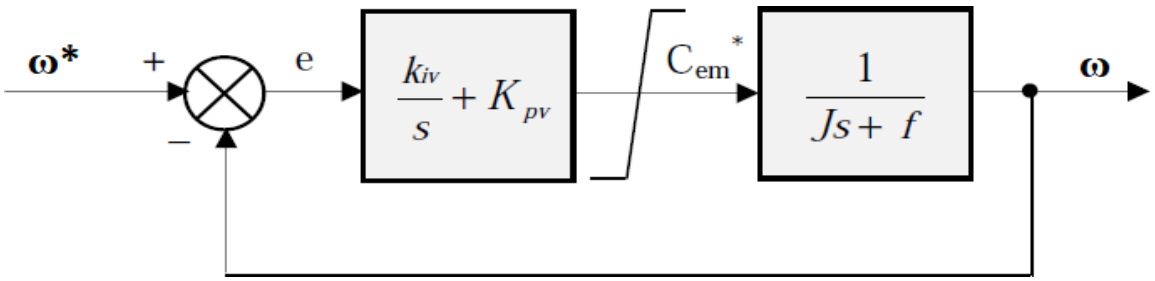

Figure III.12: Speed regulation block.

Following the same steps as in the previous calculation, we find:

$$K_{pv} = \frac{j}{r} \quad \text{(III.44)}$$

$$K_{iv} = \frac{f}{r} \quad \text{(III.45)}$$

We take: $r = r_r$.

The command must be limited by a saturation device defined by :

$$C_{em}^* = C_{em}^* si|C_{em}^*| \le C_{em}^{max} \quad C_{em}^{max} \text{signe}(C_{em}^*) \text{Si}|C_{em}^*| \ge C_{em}^{max} \quad \text{(III.46)}$$

III.12 Field weakening block:

The principle of this method consists in directly determining the component of the rotor flux from the mechanical speed of rotation of the rotor using a speed sensor, this is achievable for a de fluxing block defined by the following nonlinear function[41].

$$\emptyset_{rref} = \emptyset_n \text{si}|\Omega| \le \Omega_n \quad \text{(III.47)}$$

$$\emptyset_{rref} = \emptyset_n = \frac{\Omega_n}{\Omega} \text{si}|\Omega| > \Omega_n \quad \text{(III.48)}$$

It is schematized by the following figure:

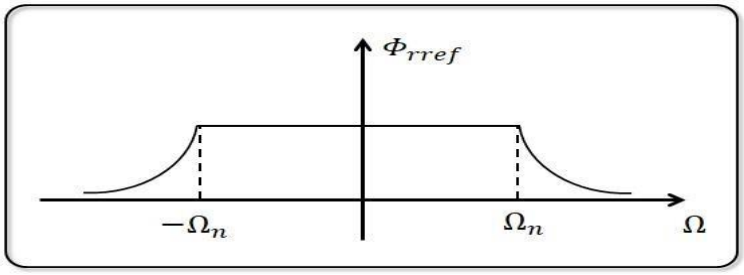

Figure III.13 : Field weakening scheme

The flux is generally kept constant at its nominal value, for rotor speeds less than or equal to the nominal speed of the machine w_n, for higher speeds the flux decreases when the speed increases in control to limit the voltage at the terminals of the machine.

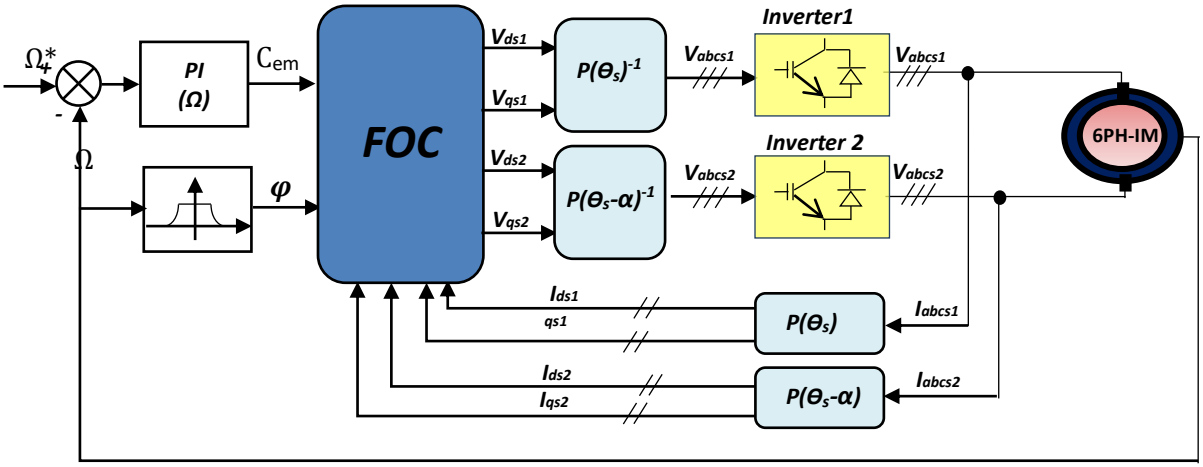

Figure III.14: Field oriented control of the 6PH-IM

II.13 Simulation and interpretation of results :

The evolution of 6PH-IM characteristics with speed regulation by the indirect method, with the application of loads *Cr* = 14Nm respectively between time intervals *t* = [1,1.5] set Cr=-14Nm danst= [3.25,3.75] s, followed by the inversion of the latter by 314 à−314à from the time *t* = 1.65*s*. it shows that:

At start-up and during empty operation, the speed (w(rad/s)) reaches the setpoint = 0.73*s*. Le electromagnetic torque(Cem (N.m)) reaches the maximum value of 54.5*N.m* à*t* = 0.049*s*, subsequently, at the beginning of the permanent regime (à*t* = 0.75*s*). Then it stabilizes throughout due to friction (close to 0).

The stator currents (stars 1 and 2) observe an input current of about 2 times the nominal current, and then during the steady state they evolve in a sinusoidal way. The current in quadrature ($i_{qs1}(A)$) developing the same pattern as the electromagnetic couple.

the stator current ($i_{qs1}(A)$) reached approximately 15A during regimetransitory, and stabilized at 0s steady state. The rotor flows progress in a manner similar to that of the electromagnetic torque during the transient speed, however they stabilize and evolve according to their instructions during the permanent speed.

The application of the load Cr = 14N.m (engine operating) during the interval detemps t = [1, 1.5] s, increases in electromagnetic torque, stator currents and rotor current, which stabilize at Cem=14N.m

i_{as1}=i_{as2}=6.2A, i_{qs1}= 7A eti_{ar}= 12A, and for the application of the load Cr = -14N.m (engine operating) during the interval detemps t = [3.25,3.75]s, on a le couple qui se stabilize respectively at Cem=-14N.mi_{as1}=i_{as2}=6.2A, i_{qs1}=-7A. Speed and rotor flows remain fixed as they continue instructions. However, in motor operation the voltage (v_{as1}(V)) and current (i_{as1}(*A*)) are almost in phase and of the same sign, which means that the power is of positive sign, that is, the machine absorbs active and reactive energy from the source, necessary for the supply of the load and for its magnetisation, which still results in the phase shift backwards (inductive effect) current to voltage.

On the other hand, the inversion of the 314 à−314*rad/* s from the moment t = 1.65*s*. The results obtained clearly show that: the speed perfectly follows its set and reverses after 1.1*s*. This leads to an increase in the current of the same magnitude as observed during the initial transitional regime, which stabilizes after 1.12*s*, to give rise to sinusoidal forms of constant amplitude. The electromagnetic torque reaches −14*N*. As the speed reverses, which stabilizes, the speed reaches its referencing value. The current i_{qS1}(*A*) evolves in a couple-like manner. Rotational flows along both axes show a slight disturbance during the inversion of speed.

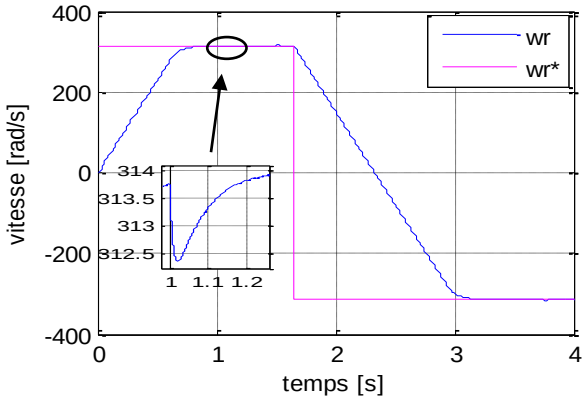

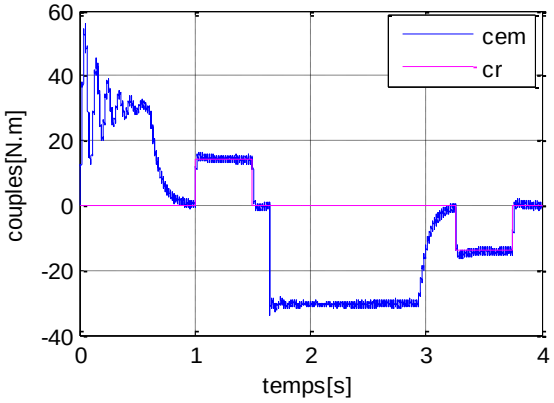

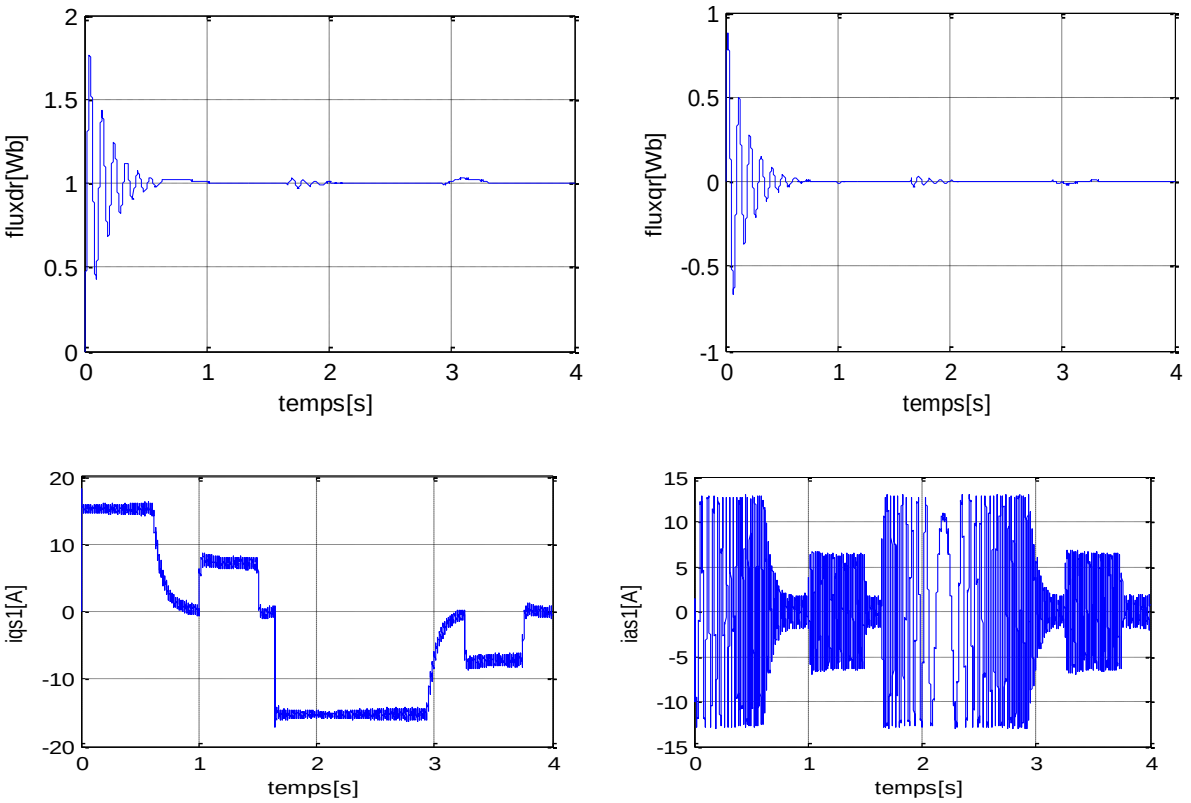

Figure III.15: Speed control of the 6PH-IM by indirect method

III.14 Conclusion:

This chapter is devoted to the vector control by orientation of the rotor flux of the six phase induction machine, the objective being the regulation of the speed by the indirect control. However, the study of the latter led us at best to highlight the characteristics of the vector control on the 6PH-IM. In control to optimize the performances of the 6PH-IM, multilevel converters are proposed to replace the classical two-level converters in the next chapter.

CHAPTER IV

Performance Optimization of the
6PH-IM by Multilevel Converters

IV.1 Introduction:

Power-electronic inverters are becoming popular for various industrial drives applications. In recent years also high-power and medium-voltage drive applications have been installed To overcome the limited semiconductor voltage and current ratings, some kind of series and/or parallel connection will be necessary. Due to their ability to synthesize waveforms with a better harmonic spectrum and attain higher voltages, multi-level inverters are receiving increasing attention in the past few years . However, the increasing number of devices tends to reduce the overall reliability and efficiency of the power converter. On the other hand, solutions with a low number of devices either need a rather large and expensive LC output filter to limit the motor- winding insulation stress, or can only be used with motors that do withstand such stress.

IV. 2 Multilevel converter driven applications

Multilevel converters are considered today as a very attractive solution for medium voltage high power applications. In fact, several major manufacturers commercialize NPC, FC or CHB topologies with a wide variety of control methods, each one strongly depending on the application. Particularly the NPC has found an important market in more conventional high power ac motor drives applications like conveyors, pumps, fans and mills among others, which offer solutions for industries including oil and gas, metals, power, mining, water, marine and chemistry.

The back to back configuration for regenerative applications has been also a major hit of this topology, used for example in regenerative conveyors for the mining industry, or grid interfacing of renewable energy sources, like wind power. On the other hand FC converters have found particular applications for high bandwidth high switching frequency applications such as medium voltage traction drives. Finally the cascaded H-bridge has been successfully commercialized for very high power and power quality demanding applications up to a range of 31MVA, due to its series expansion capability. This topology has also been reported for active filter and reactive power compensation applications, electric and hybrid vehicles, photovoltaic power conversion, uninterruptible power supplies, and Magnetic Resonance Imaging. As an example of a commercial multilevel power converter a 34kV-15MW three-phase six-cell CHB converter from SIEMENS for regenerative drives is shown in A summary of multilevel converter driven applications is illustrated [42] .

IV.3 Asymmetric and Hybrid Multi-Level Inverters

Asymmetric multi-level inverters use different intermediate-circuit capacitor voltages in various parts of the inverter. By addition and subtraction of these voltages, more different output-voltage levels can be generated with the same number of components, compared to a symmetric multi-level inverter. Higher output quality can be obtained with smaller circuit and control complexity, and output filters can be remarkably shrunk or even eliminated.

The various parts of an asymmetric multi-level inverter execute different functions in the power conversion. Equipped with several different semiconductor devices, a hybrid converter exploits their individual advantages and strengths. The main power is supplied with high reliability and low losses by one device, the output harmonic content is reduced by another. By using state-of-the-art semiconductor devices, this can lead to a better overall design for medium-voltage drives.

In order to further simplify the power part and increase the efficiency of such a converter, we can remove some of the power supplies and let those parts of the converter supply only reactive power. We obtain a very interesting solution in terms of power quality, efficiency, reliability and cost.

However, the resulting system is unstable, and without control the non- supplied intermediate-circuit capacitor voltages will quickly run away from their nominal values. An appropriate converter control method is needed to stabilize those voltages, preferably without deteriorating the output voltage. In general, this cannot be done instantaneously by lack of an equilibrium state, but only on an average in time. Apart from normal operation, also the pre- charging of the non-supplied intermediate-circuit capacitors upon converter start-up is an issue to consider[43].

IV.4 Multilevel static converters

Multi-level static converters offer huge advantages over 2-level inverters. These advantages are visible from both a technological and functional point of view [44] :

- **Technological advantages**: In multi level static converters, the voltage distribution is obtained in a natural way at the set speed, allowing each semiconductor to be switched independently of the others. This makes the converter more robust and

more efficient during switching. The voltage switched is of reduced amplitude and the switching is therefore easier to manage.

- **Functional advantages for the converter:** Possibility to access higher power applications. Better compromise between static performance (saturation voltage) and dynamic performance (switching time, switching losses, switching frequency).
- **Functional advantages for the machine:** The number of voltage generated by a multi-level static converter is higher than that of the static converter at 2-voltage levels, which improves the quality of its waveform, which will result in a reduction in its harmonic distortion. This can lead to considerable advantages, such as a reduction in iron losses, an increase in the life of insulators or a reduction in electromagnetic radiation from machine windings.

Below, we briefly present the main topologies of the multi-stage static converters mentioned in the literature.

IV.5 Multilevel topologies

It is a fact that, until today, multilevel topologies are the best alternative to implement low-frequency based inverters with low output voltage distortion. This chapter makes a review about most common multilevel topologies and shows which ones are more suitable to implement inverters for SARES[45].

The multilevel concept and notation.

A multilevel inverter can be defined as a device that is capable to produce a stepped waveform. The generalized stepped waveform is shown in figure 1.Usually, and also in this work, the follow definitions apply:

p:number of steps in a quarter-cycle;

2*p + 1: number of levels of a converter

4*p:number of steps of a converter.

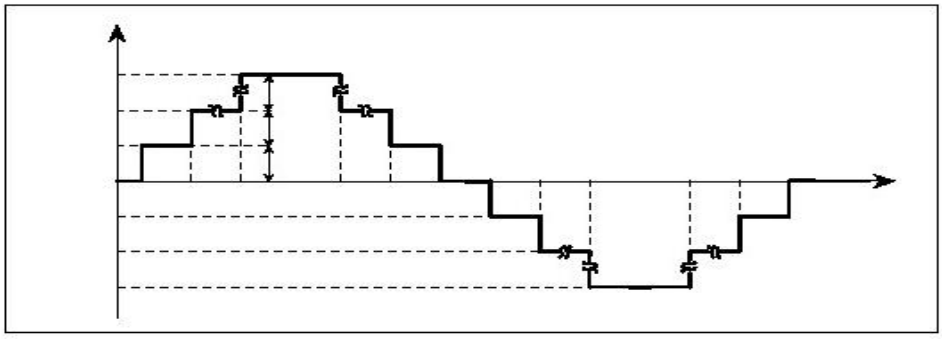

Figure IV.1: The generalized stepped waveform is shown

IV.6 Types of Multilevel Inverter:

Multilevel inverters are three types.

IV.6.1 Cascaded H-Bridge Multilevel Converters

A single H-bridge structure is capable of producing three voltage levels, namely $+U_{dc}$,0,$-U_{dc}$. A series connection of these individual bridges yields a staircase output waveform wherein each step corresponds to each individual bridge. To obtain higher levels in the output waveform, more H-bridges need to be connected. Typically for an n level converter, (n-1)/2 H-bridges are required per phase. Some of the advantages associated with this topology are summarized below [46]:

- It requires the least number of components compared to the other topologies for thesame voltage level required.
- It possesses a modularized circuit layout and does not require any extra diodes orclamping capacitors.

The disadvantage of such a topology is the requirement of separate DC sources hence makingit difficult for extending to higher levels.

A single phase of an n- level cascaded H-bridge structure with separate DC sources is shown in FigureIV.2.

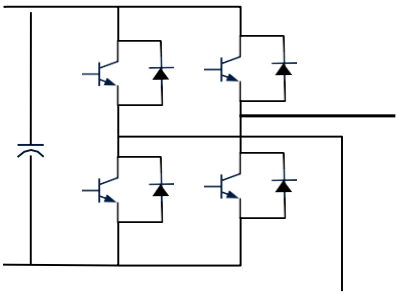

Figure IV.2: Single phase cascaded H-Bridge structure

IV.6.2 Flying Capacitor Multilevel Converters

In 1992 the Flying capacitor converter was introduced for the first time. The work of Meynard and Foch upgrades the technique where series connection of switches was needed, adapting the system to higher voltage conversions. High-voltage conversion requires semiconductors capable of keepingthe desired voltage at a certain level. The paper shows positive results, such as control simplicity and a more desirable output waveform. Other studies also show that the flying capacitor converter shows good performance for high and low modulation index [47].

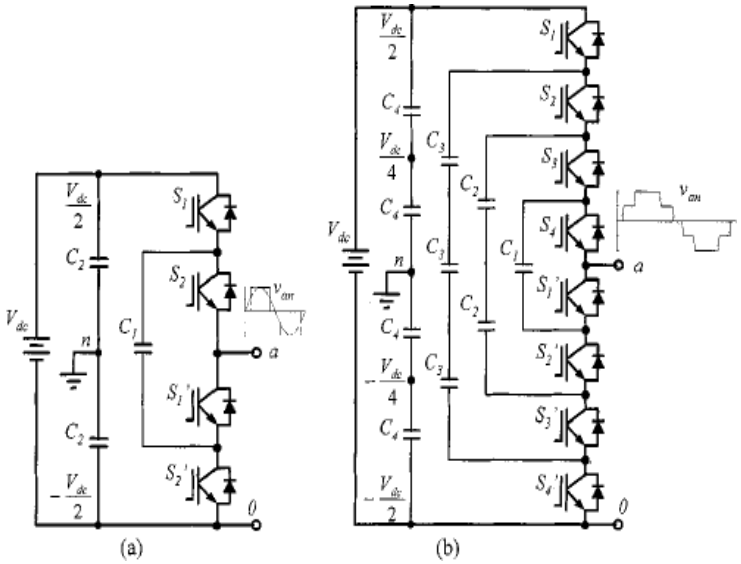

Figure IV.3 : Circuit of a Flying Capacitor (a) two-level converter for one phase leg(b) three-level converter for one phase leg

IV.6.3 Diode Clamped Multilevel Converters

The diode clamped multilevel inverter has almost the same structure as the flying capacitor, but instead of capacitors this inverter type uses diodes as clamping devices, creating the desired output voltage. The voltage across each capacitor is defined as $V_{DC}/(m-1)$, m being the number of levels and $(m-1)$ the amount of capacitors needed. So, for a two-level inverter the voltage is V_{DC} and for that case one capacitor is used. For a three-level inverter the voltage is $V_{DC}/2$ and therefore is in need of two capacitors. This specific design makes it possible to increase the number of levels just by increasing the amount of capacitors. In this context the terminology "neutral point clamped" is often used. It describes the neutral point between two capacitors connected across the DC-bus adding an extra level to the system. If m is an even number, the neutral point is not utilized, so then it is usually called a multiple point clamped converter. Experience show that higher levels than the three-level converter causes voltage balancing problems, so it is common to use the three- level inverter, but there are studies demonstrating SVPWMs with self balancing systems[47].

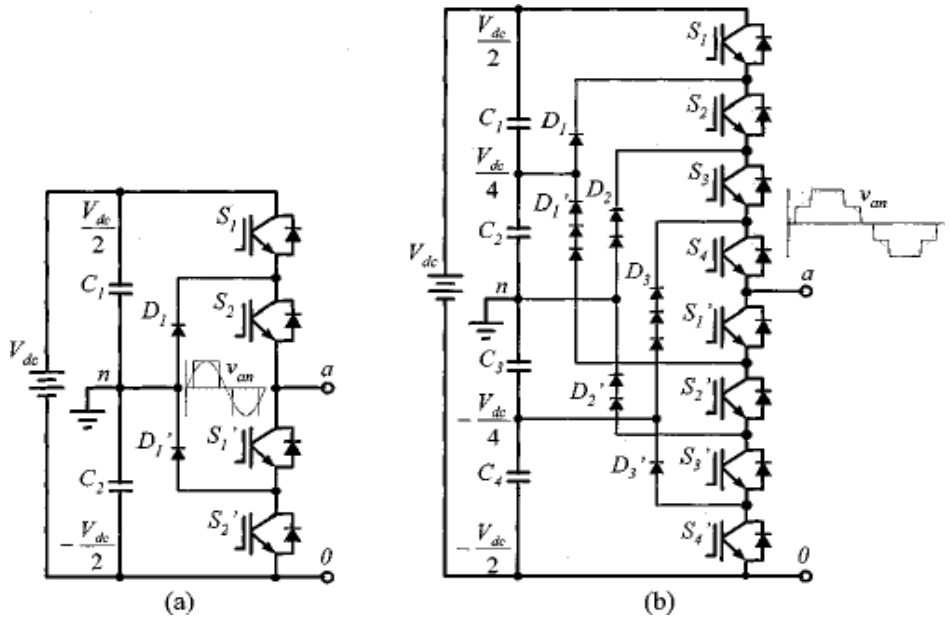

Figure IV.4: A Diode Clamped converter for a (a) three-level inverter (one phase leg) andfor (b) five-level inverter (one phase-leg)

IV. 7 Modular multilevel converter

The modular multilevel converter (MMC) was first proposed for high voltage applications by Dr. Lescinar in . The MMC is a three-phase converter composed of low voltage semiconductor valves that can be manipulated to behave like controlled voltage sources in medium and high voltage applications. The MMC is a scalable technology with many advantages over more conventional two and three level voltage source converters (VSCs). Its modular topology allows for scalability of medium to high voltage ranges, as well as for control of harmonic distortion by varying the number of sub modules used in the design. This converter topology also allows for lower switching frequency requirements, which significantly decreases the converter's switching losses. Modular multilevel converters are also suitable for use in interfacing renewable energy power sources to the conventional AC grid [48].

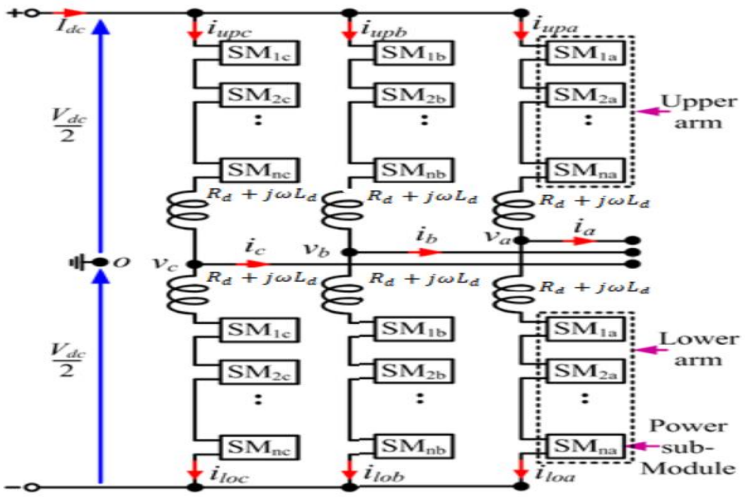

Figure IV.5: A Diode Clamped converter

IV.8 Generalized Multilevel Inverter

The generalized structure was introduced by Peng in 2001 (Peng, 2001). This topology has ability to balance the capacitor voltage itself. As it is illustrated in FigureIV.6, this configuration can be expanded easily and generate more levels while self-balancing the voltage.

Being symmetrical allows deriving many other configurations from this complete configuration e.g. NPC and FC. On the other hand, using too many switches and capacitors is a limitation of this topology. However, it is a good reference of switch combinations to study and analyze the multilevel inverter structures that can result in proposing new topologies withless components and self-voltage-balancing feature[49].

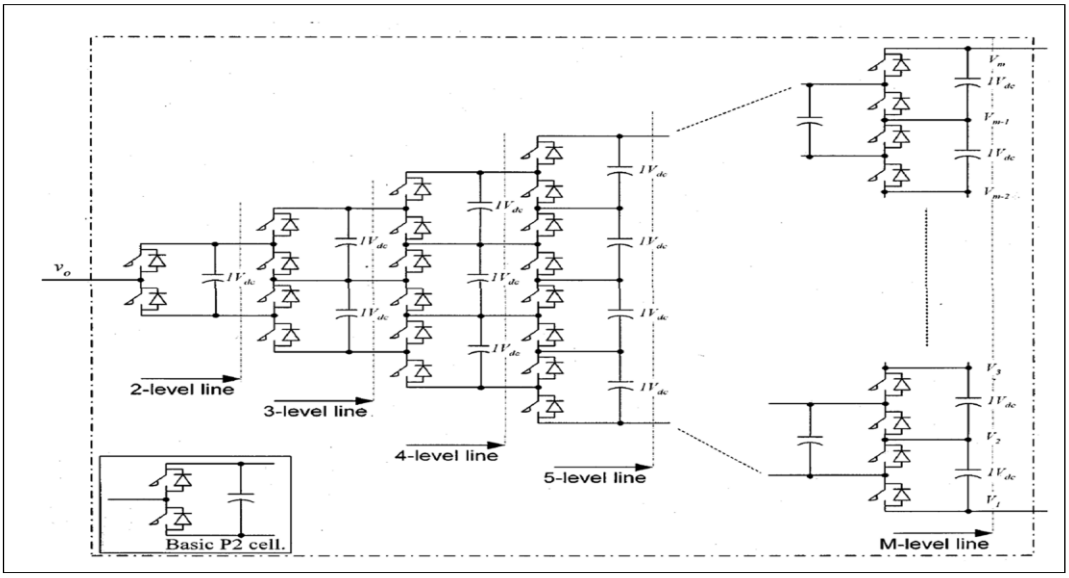

FigureIV.6: Generalized multilevel inverter topology

IV.9 NPC Structure 3-Level UPS Overview

The three-stage NPC three-phase static converter in Figure IV.7 has two DC voltage sources and three symmetrical arms. Each arm is made up of four pairs (diode - GTO), each representing a bidirectional switch and two middle diodes, allowing to have the zero level of the inverter output voltage. This structure requires the use of controllable switches at initiation and blocking.

The N.P.C structure uses two input voltages: UC1 and UC2. It consists in creating a middle point on the E-value DC voltage stage (UC1+UC2 = E), allowing to generate amplitude - E/2, 0, +E/2 whose combination makes it possible to have a wave closer to the sinusoid than with the conventional two-stage inverter structure.For an input voltage E, the switches of a three-tier UPS support half the voltage of a two-tier UPS.[50].

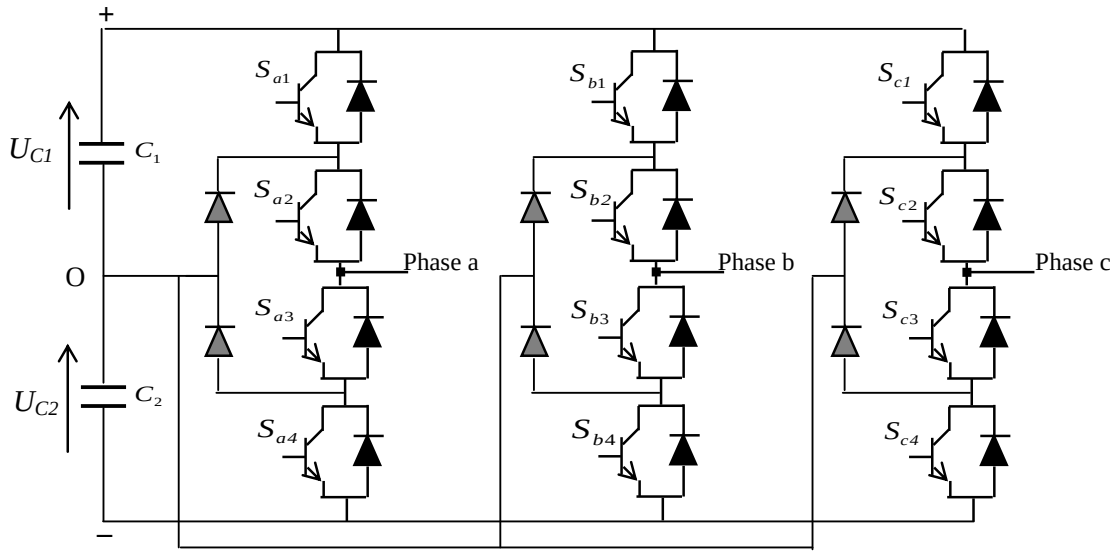

FigureIV.7 : Electrical diagram of the three-phase static converter with NPC structure.

This structure called neutral point "clamped" is one of the structures of static converters at 3 voltage levels. It has many advantages, such as the number of voltage generated is higher, less distortion harmonic and low switching frequency [51].

By combining the four switches of the same arm, 24 possible sequences are obtained. Only three sequences are functional, the others cause either short circuits of the DC voltage sources, or disconnection of the load [52].

Figure IV.8 shows the NPC type inverter bar configurations corresponding to the following three functional sequences:

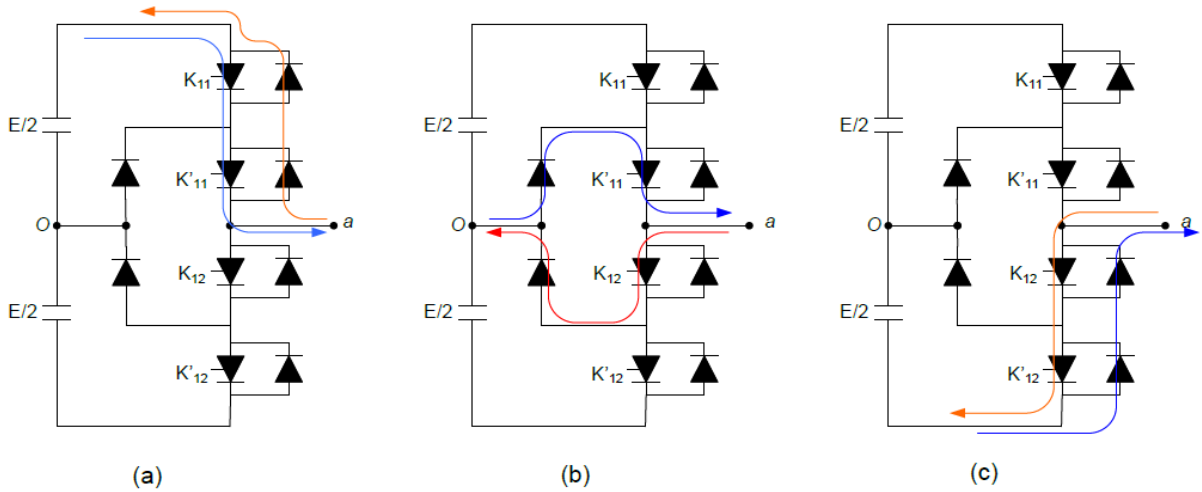

Figure IV.8: Functional sequences of a three-phase static converter arm.

An arm (k) of the three-stage static converter can be represented by a switch (S_k) in three states:

- $S_k = -1$ for the configuration C_0 ; $V_{kM} = -U_c \Longrightarrow$ [0 0 1 1] : switches k_{12}, k'_{12} are closed and k11, k'11 are open, if the energy transfer is done from the AC side to DC the current goes through the thyristors k12 and k'12, if the opposite goes through D'1 and D'2.
- $S_k = 0$ for the configuration C_1 ; $V_{kM} = 0 \Longrightarrow$ [0 1 1 0] : switches k'_{11}, k_{12} are closed and k_{11}, k'_{12} are open, if the energy transfer is done from the AC side to DC the current goes through the thyristor k12 and the diode D'c1, otherwise it goes through the k'_{11} et D_{c1}.
- $S_k = 1$ for the configuration C_2 ; $V_{kM} = U_c \Longrightarrow$ [1 1 0 0] : switches k_{11}, k'_{11} are closedet k_{12}, k'_{12} are open, if the energy transfer is done from the DC side to AC the current passes through the thyristors k_{11} et k'_{11}, If not, it goes through D1 and D2.

The control of the switches and the voltages at the output of an inverter arm are given by the following table:

Configuration	K_1	K_2	K_3	K_4	S_k	Tension à la sortie d'un bras *k* par apport au point milieu *M*
C_0	0	0	1	1	-1	$V_{kM} = -U_c$
C_1	0	1	1	0	0	$V_{kM} = 0$
C_2	1	1	0	0	1	$V_{kM} = U_c$

Tableau IV.1 : Electrical quantities of a three-stage static converter k-arm.

The voltages at the converter output relative to point (n) are:

$$\begin{bmatrix} V_{an} \\ V_{bn} \\ V_{cn} \end{bmatrix} = \frac{1}{3}\begin{bmatrix} 2 & -1 & -1 \\ -1 & 2 & -1 \\ -1 & -1 & 2 \end{bmatrix}\begin{bmatrix} V_{aM} \\ V_{bM} \\ V_{cM} \end{bmatrix} \quad \text{(IV.1)}$$

We have: $V_{kM} = S_k.U_c$ (V.37)

By replacing the voltages with their expressions, the simple voltages applied to the machine become:

$$\begin{bmatrix} V_{an} \\ V_{bn} \\ V_{cn} \end{bmatrix} = \frac{U_c}{3}\begin{bmatrix} 2 & -1 & -1 \\ -1 & 2 & -1 \\ -1 & -1 & 2 \end{bmatrix}\begin{bmatrix} S_a \\ S_b \\ S_c \end{bmatrix} \quad \text{(IV.2)}$$

voltage vector depending on the sequences and the continuous source is : The voltage vector according to the sequences and the continuous source is:

$$V_s = \sqrt{\frac{2}{3}}\left(V_{an} + a.V_{bn} + a^2.V_{cn}\right) = \sqrt{\frac{2}{3}}\left(S_a + a.S_b + a^2.S_c\right)U_c \quad \text{(IV.3)}$$

Previous relationships show that there are twenty-seven (33=27) switching states for the UPS. Depending on these states, there will be 19 different VS voltage vectors in the module. The representation of these vectors, Figure (V.20), shows that they are classified into four groups according to their modules[52]. We distinguish then: The vector voltage null Vz, the small voltage vectors (V1S,V2S, V3S, V4S, V5S, V6S,), the medium voltage vectors (V1M, V2M,V3M,V4M,V5M,V6M,), and the large voltage vectors (V1L, V2L,V3L,V4L,V5L,V6L,).

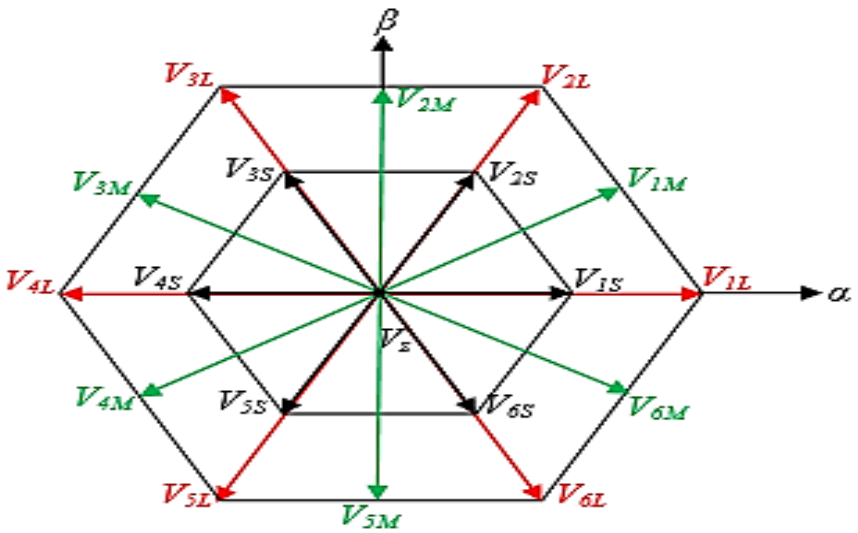

Figure IV.9 : Diagram of the voltage vector V_s in the mark $\alpha\beta$.

Table (IV.2) below shows the classification of stress vectors in four groups according to their amplitudes:

group of vectors	Voltage vector V_s (S_a, S_b, S_c)
Large Vectors (Large Vectors)	V_{1L}(1,-1,-1) ; V_{2L}(1,1,-1) ; V_{3L}(-1,1,-1) V_{4L}(-1,1,1) ; V_{5L}(-1,-1,1) ; V_{6L}(1,-1,1)
Means vectors (Middle Vectors)	V_{1M}(1,0,-1) ; V_{2M} (0,1,-1) ; V_{3M}(-1,1,0) V_{4M}(-1,0,1) ; V_{5M}(0,-1,1) ; $V_{6M(}$1,-1,0)
Small Vectors	V_{1S}[(1,0,0) (0,-1,-1)] ; V_{2S}[(1,1,0) (0,0,-1)] V_{3S}[(0,1,0) (-1,0,-1)]; V_{4S}[(0,1,1) (-1,0,0)] V_{5S}[(0,0,1) (-1,-1,0)] ; V_{6S}[(1,0,1) (0,-1,0)]
Zero Vectors	V_Z[(1,1,1) (0,0,0) (-1,-1,-1)]

Table IV.2 : Groupe des vectrices tensions.

IV.10 Control strategies for three-tier static converters

Voltage inverters can be controlled according to several strategies. At low frequencies, they will be controlled in full wave; the control signal will be at the same frequency of the desired voltage at the output and the continuous source must be adjustable (using a thyristor rectifier or chopper). At high frequency, they will be controlled in pulse width modulation. This allows you to adjust both amplitude and frequency by keeping the continuous source constant (diode bridge). In order to produce an output voltage close to the sinusoid, different strategies of pulse width modulation have been proposed such as: triangulo-sinusoidal modulation, Current hysteresis control and vector modulation. Here we are interested in the first technique.

- **Control by sinus-triangle modulation**

The general principle of control by PWM sinus-triangle has been introduced in section (III.4.1). a)). The basic diagram of this technique applied to the three-stage static converter is given in the figure (IV.10).

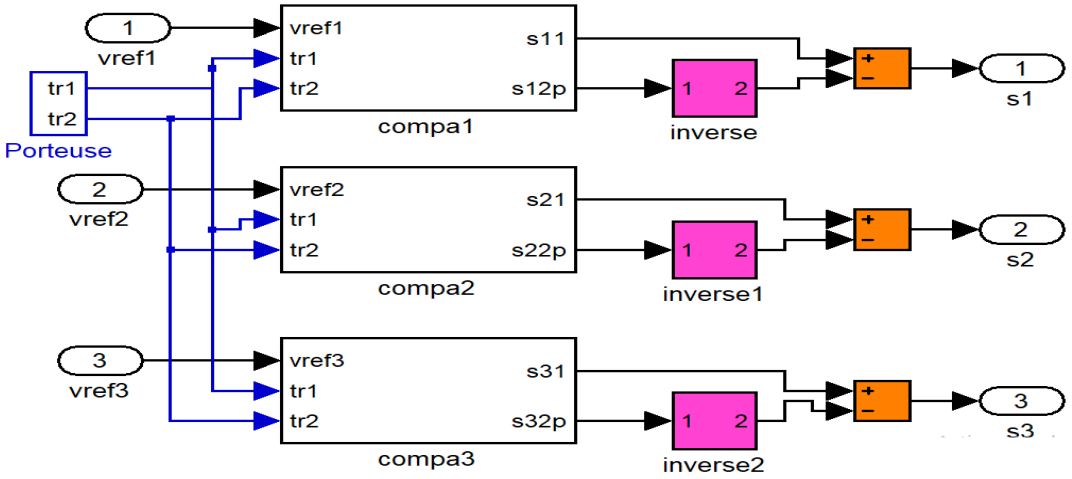

Figure IV.10 : Dual-carrier PWM control of a three-phase NPC static converter.

To generate the PWM-ST control pulses of the three-phase static voltage converter, two triangular carriers are required. These carriers have the same frequency fp and amplitude Up. They are then compared to the reference signal (sinus) of amplitude Ur and frequency. Each comparison gives 1, if a carrier is greater than or equal to the reference, 0 otherwise. Thus, the control signals of the switches of the first arm (T12, T13) and (T11, T14), the second arm (T22, T23) and (T21, T24), and the third arm (T32, T33) and (T31, T34) are complementary.

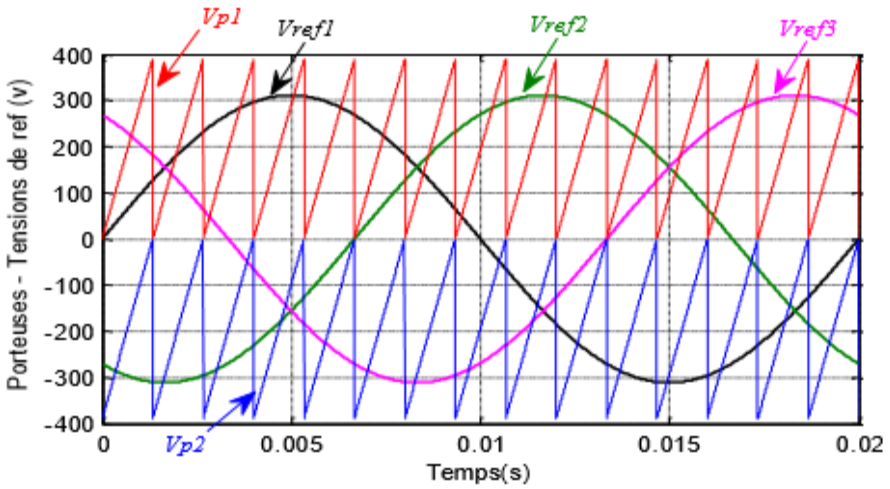

Figure IV.11: The three reference voltages with two unipolar carriers.

IV.11 Simulation and interpretation of results

To validate the proposed algorithm, we present in this part the results of numerical simulation illustrating the performance of vector control with 6PH-IM multi-level converters. We have placed the 3-level converter under the same conditions as the previous

case with 2-level converters, namely: the sampling period Te, the gains of the current and speed controllers and the input voltage of the converter. The simulation results in Figure V.23 show the high performance of the proposed FOC-3N strategy.

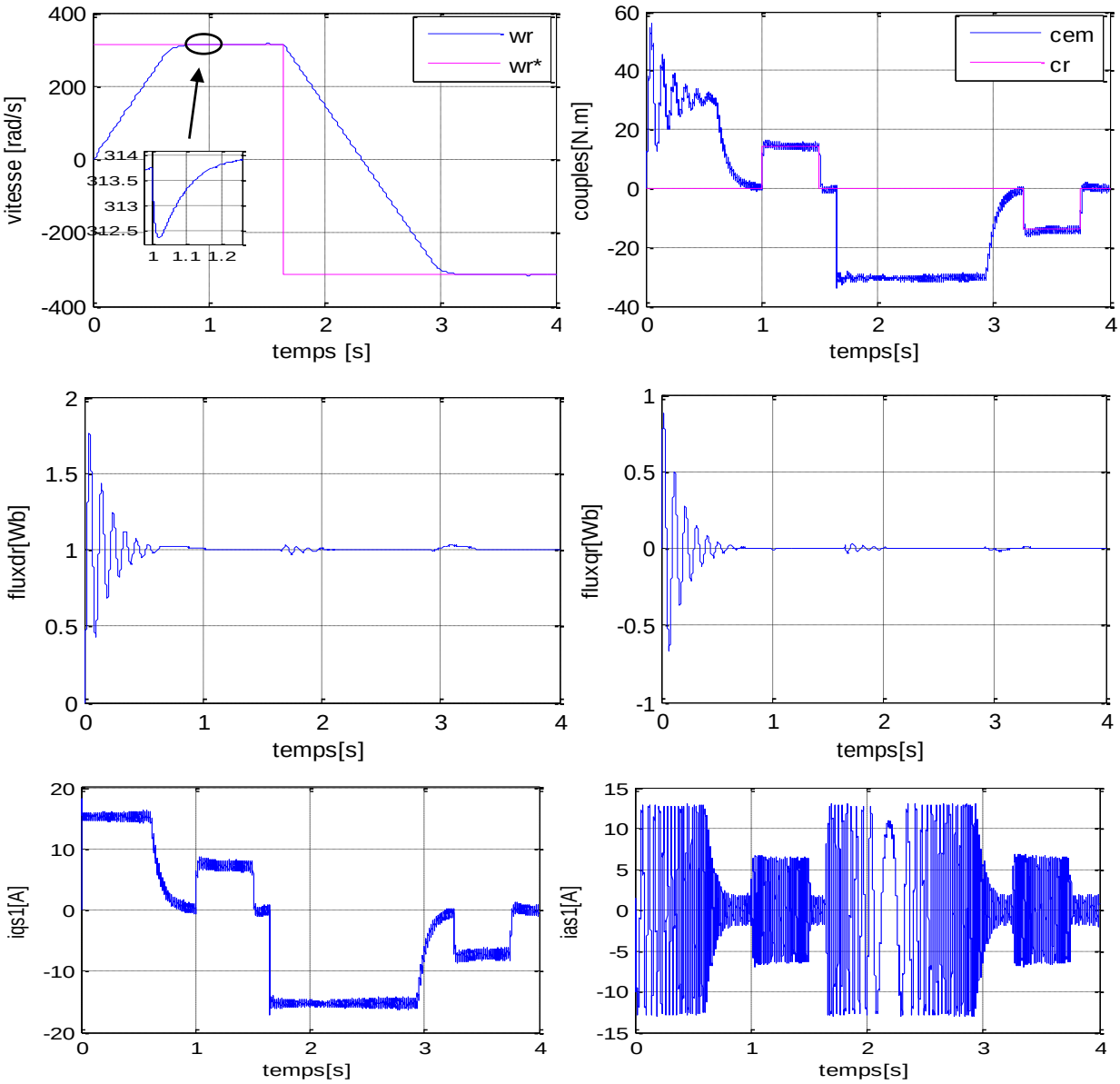

Figure IV.12: Speed control by indirect method based on three-level converters

IV.12 Performance comparison between the two-level and the three level converters

Figure IV.13 shows that in the case of FOC-3N, good torque and current performance is achieved with fewer oscillations. Figure IV.13-b shows that using the 3-level UPS will decrease the stator current ripples, and in the established regime the current becomes purely

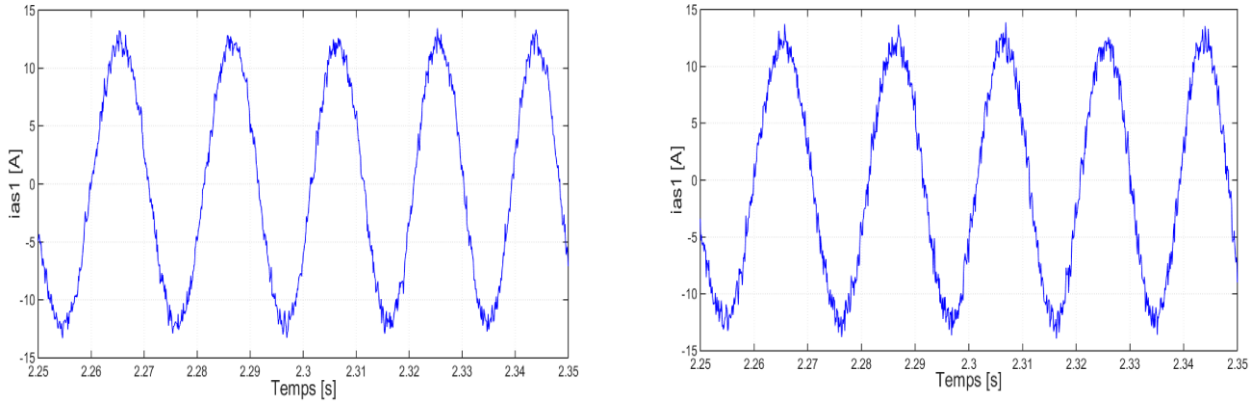

(a) (b)

Figure IV.13: Current signal of phase a: (a) with 2-level converter,(b) with 3-level converter

Fondamental (50HZ), THD=4.02% Fondamental (50HZ), THD=2.25%

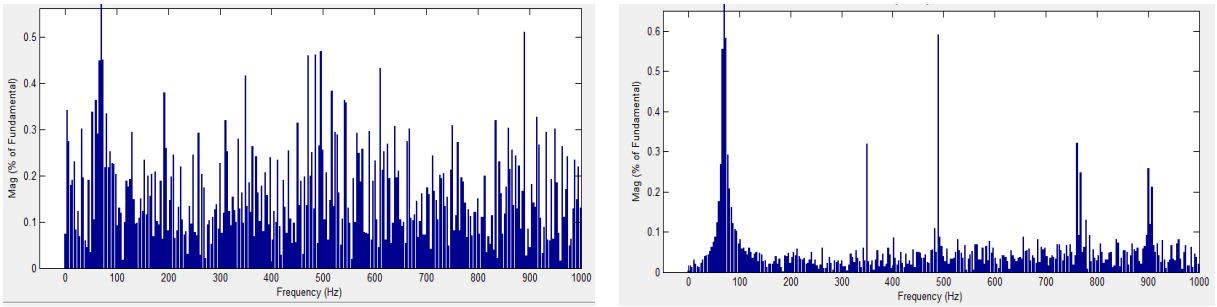

Figure IV.14 : Harmonic analysis of current spectra: (a) with 2-level converters,(b) with 3-level converters.

From the results in Figure V.14 it can be seen that the total harmonic distortion of the currents is considerably reduced compared to the FOC-2N. So the use of multi-level inverters in general improves some of the performance of the conventional FOC, such as torque and flow ripples.

IV.13 Conclusion

In this chapter, we studied the multi-level inverters and the types of topology, and a comparison was made between the three-level and the two-level, and we noticed that the higher level provide better output voltage and the less desirable the amplitude of harmonics, and we conclude from that that the three level is better than the two level in terms of control.

General Conclusion

The work presented in this thesis exposes the synthesis of a reliable and high-quality control technique, for the speed regulation of a six-phase induction machine (6PH-IM), once by vector control based on two-level converters and another time based on multi-level converters. The main objective of this thesis is to improve the control performance in terms of quality, reliability and accuracy. This study was made in four chapters:

In the first chapter, we examined the six phase machines and their properties, and discovered that they are the typical example of these machines. In which, the six phase machine offers a good technical and economic compromise for high energy applications such as pumps, fan, cement plants etc.

In Chapter II, our efforts were dedicated to the modeling of the 6PH-IM, the model that describes the equations of 6PH-IM was developed in the vertical and horizontal axis system thanks to the Park conversion matrix. Remember that the study was conducted at a shift angle of 30 degrees between the two stars.

Chapter III provides indirect control of the vectors of the six-phase induction machine, whose principle is to have a torque similar to that of the DC device. To do this, we base on the indirect rotor flow guideline that is applied to control speed using two traditional PI-type regulators, and then the device is attached to two voltage converters controlled by the PWM pulse width modulation technology, which produces torque harmonies, but it remains low compared to traditional three-phase machines.

In the last chapter, we studied multilevel converters in order to improve control performance. We have compared the three and the two-level converters. From the obtained results, it can be noticed that the three levels converter provides better results than the two-levels in terms of control quality and reliability.

After consulting the obtained results from chapters three and four, it is possible to envisage interesting perspectives and practical developments that could help to exploit this machine better:

- Using other multi-level converters topologies;
- Application of other robust control techniques, such as fuzzy logic, predictive control, neural networks, genetic algorithms, etc.

-Finally, experimental validation in real time of the proposed methods.

Annexe

►D.1 - Paramètres de la machine asynchrone à double étoile :

Symbole of parameters	Numerical value
Rated Power P_n	4.5 KW
Rated current I_n	6.5 A
Rated voltage V_n	220/380 V
Rated frequency f_n	50Hz
Résistances statorique R_{s1}, R_{s2}	3.72 Ω
Résistance rotorique R_r	2.12 Ω
Inductance statorique L_{s1}, L_{s2}	0.022 H
Inductance rotorique L_r	0.006H
Inductance mutuelle L_m	0.3672 H
Coefficient de frottementfv	0,001 Nm s/rd
Tension du bus continu U_{DC}	1200V
Moment d'inertie J	0.0625 kg.m^2
Nombre de paires de pôles p	1

REFERENCES

[1] Z.M.N.ZOUAOUID and **M.T.MESSAI**, « Commande Vectorielle de la Machine à Double Stator », Mémoire Master, Université Larbi Ben M'Hidi Oum EL Bouaghi, 2018.

[2] BERRABAH Fouad, « Commande Sans Capteur De La Machine Asynchrone », Thèse De Doctorat De l'Université BADJI MOKHTAR – ANNABA, 2016.

[3] RAHAL HILAL, « Commande non Linéaires Hybrides et roboustes de la Machine Asynchrone Double Etoile», Théses de Doctorat, Université Mohamed BOUDIAF De MSILA 2020.

[4] D. Hadiouche, « contribution à l'étude de la machine asynchrone double étoile : modélisation, alimentation et structure», Thèse de doctorat de Université Henri Poincaré, Nancy-1., soutenue 20 décembre 2001

[5] D.Hadiouche and **H.Razik** and **A.Rezzoug,** « Modelling of a double-star induction motor with an arbitrary shift angle between its three phase windings » , EPE-PEMC2000, Kosice

[6] M. Bernard, « Historique des machines électromagnétiques et plus particulières des machines a réluctance variable», Revue 3E .In˚3. pp. 3–8, Juin 1995.

[7] H.AMIMEUR, « Contribution à la Commande d'une Machine Asynchrone Double Etoile par Mode de Glissement »,Mémoire De Magister, Université El Hadj Lakhdar de Batna, 2008.

[8] Mesai Ahmed Hamza « Commandes de hautes Performances d'une Machine Asynchrone Double Etoile MASDE via des Convertisseurs Multi-niveaux » Thesis Doctorat, Université DJILLALI LIABES De SIDI-BEL-ABBES, 2019.

[9] J. Rodriguez, J.-S. Lai, and F. Z. Peng, "Multilevel inverters: A survey of topologies, controls, and applications," IEEE Trans. Ind. Electron., vol. 49, no. 4, pp. 724–738, Aug. 2002.

[10] S. Rizzo and N. Zargari, "Medium voltage drives: What does the future hold?" in Proc. 4th IPEMC Conf., Aug. 14–16, 2004, vol. 1, pp. 82–89.

[11] **R. D. Klug and N. Klaassen,** "High power medium voltage drives—Innovations, portfolio, trends," in Proc. Eur. Conf. Power Electron. Appl., 2005, pp. 1–10.

[12] B. Wu, High-Power Converters and AC Drives. New York: Wiley IEEE Press, Mar. 2006.

[13] J. Rodriguez, S. Bernet, B. Wu, J. O. Pontt, and S. Kouro, "Multilevel voltage-source-converter topologies for industrial medium-voltage drives," IEEE Trans. Ind. Electron., vol. 54, no. 6, pp. 2930–2945, Dec. 2007.

[14] P. Steimer, "High power electronics, trends of technology and applications," in Proc. PCIM, Germany, May 2007.

[15] L. G. Franquelo, J. Rodriguez, J. I. Leon, S. Kouro, R. Portillo, and M. A. M. Prats, "The age of multilevel converters arrives," IEEE Ind. Electron. Mag., vol. 2, no. 2, pp. 28–39, Jun. 2008.

[16] J. Rodriguez, B. Wu, S. Bernet, N. Zargari, J. Rebolledo, J. Pontt, and P. Steimer, "Design and evaluation criteria for high power drives," in Conf. Rec. IEEE IAS Annu. Meeting, Oct. 5–9, 2008, pp. 1–9.

[17] J. Rodriguez, L. G. Franquelo, S. Kouro, J. I. Leon, R. C. Portillo, M. A. M. Prats, and M. A. Perez, "Multilevel converters: An enabling technology for high-power applications," Proc. IEEE, vol. 97, no. 11, pp. 1786–1817, Nov. 2009.

[18] B. K. Bose, "Power electronics and motor drives recent progress and perspective," IEEE Trans. Ind. Electron., vol. 56, no. 2, pp. 581–588, Feb. 2009.

[19] ABB. [Online]. Available: www.abb.com

[20] SIEMENS. [Online]. Available: www.siemens.com

[21] TMEIC-GE. [Online]. Available: www.tmeic-ge.com

[22] Ansaldo Sistemi Industriali. [Online]. Available: www.asiansaldo.com

[23] Converteam. [Online]. Available: www.converteam.com

[24] Eaton. [Online]. Available: www.eaton.com

[25] Arrowspeed. [Online]. Available: www.arrowspeed.com

[26] Ingeteam. [Online]. Available: www.ingeteam.com

[27] H.AMIMEUR,« Contribution ou Control de la Machine Asynchrone Double Etoile »,Thése Doctorat, Université El Hadj Lakhdar de Batna, 2012.

[28] F.RJEM and **A.G.LECHAB** «Commande d'onduleur Mltiniveaux Asynchrone Application à la conduite de la Machine asynchrone Double Etoile » Mémoire Master académique, Université Kasdi Merbah de Ouargla, 2020.

[29] Y.KICHENE and **B.ZAOUALI,** « Commande Intelligante Floue d'une Machine Asynchrone Double Etoile » Mémoire présenté pour l'obtention Du diplôme de Master Professionnel, Université Mohamed BOUDIAF De MSILA, 2020.

[30] W.ABADI and **H.GABOUSSA** and **C.E.SOUSSA** and **A.HECHIFA,** « Commande Par Mode Glissant de la Machine Double Etoile » Mémoire Master académique, Université

Echahid Hamma Lakhdar d'El-oued,2022.

[31] M.BOUDIAF « Etude et Contrôle de la Machine Asynchrone Double Etoile »Mémoire Master Université Mohamed BOUDIAF De MSILA, 2013.

[32] : Fellah boumedyen «commande par mode glissant de la machine asynchrone double étoile»Mémoire de Master en Électrotechnique,Universitéde Sidi Bel Abbes, 2012

[33] : électronique de puissance 10 éditions par Guy Séguier, livre

[34] L.LATRECHE and **B.BASSOUS** « Modélsation et Simulation des Machines Electriques Triphasés à Double Etoile » Mémoire de Master académique, Université Echahid Hamma Lakhdar d'El-oued,2017.

[35] ABDE KRIM AMMAR, « Etude et Commande d'une Machine Asynchrone Double Etoile » Mémoire de Magister, Université Sétif 1, 2013.

[36] E. Merabet, « Commande Floue Adaptative d'une Machine Asynchrone Double Etoile», Mémoire de Magister, l'Université de Batna 2008.

[37] A.DJABOREI « Etude Commande de la Machine Asynchrone Double Etoile » Mémoire de Master académique, Université Kasdi Merbah de Ouargla, 2013.

[38] B.CHEBOUKI and **M.EL.A TAMRABET** « Commande Vectorielle de la Machine à Double Stator par les Techniques de L'intelligence Artificielle », Mémoire de Master académique, Université Larbi Ben M'Hidi Oum EL Bouaghi, 2021.

[39] S.DERDOURI and **A.H.ZEBIDI** and **M.REHOUMA,** « Modélisation et Commande de la Machine Asynchrone Double Etoile », Mémoire de Master académique, Université Echahid Hamma Lakhdar d'El-oued,2022.

[40] N.BELFAR and **A.RAHLI** « Amélioration des Performances d'une Commande à Base de Mode Glissant d'une Machine Asynchrone Double Etoile », Mémoire de Master académique, Université Mohamed BOUDIAF De MSILA, 2021.

[41] R.DOUMI « Commande PI Flou d'une Machine Asynchrone Double Etoile », Mémoire présenté pour l'obtention Du diplôme de Master Académique, Université Mohamed BOUDIAF De MSILA, 2019.

[42] Z.BENAISSA and **S.BENNENI** « Commande Véctorielle de la Machine Asynchrone Double Etoile », Mémoire de Master académique, Université Mohamed BOUDIAF De MSILA, 2008.

[43] LEOPOLDO G.FRANQUELO « The Age of Multilevel Converters Arrives »,

[44] MARTIN VEENSTRA « Investigation and Control of A hybrid Asymnetric Multi-level Inverter for Medium Voltage Application», Memoire Master, LAUSANNE, EPFL 2003.

[45] S. El Aimani, « Modélisation de différentes technologies d'éoliennes intégrées dans un réseau de moyenne Tension», Thèse de Doctorat, France: L2EP Ecole central de Lille, 2004.

[46] T.SUNEEL «Multilevel Inverters :A Review Report », International Journal, Jan. 2014.

[47] CARLOS CASTILLO BONILLA and **SHWETA MERILYN TIGGA** « Design and performance comparison of Two-level and Multilevel Converters for HVDC Applications », Master's Thesis in Electric Power Engineering, University CHALMERS, Göteborg, Sweden, 2011.

[48] BENGI TOLUNOY « Space Vector Pulse Width Modulation for Three-Level Converters», Master Programme in Electrical Engineering University UPPSALA, February 2012.

[49] JORDAN D.ROGERS «Comparative Analysis Of Current Control Methods For Modular Multilevel Converters», Thesis Master, University of South Carolina, 2016.

[50] HANI VAHEDI « Modeling, Development and Control of Multilevel Converters for Power System Application », Thesis Ph.D, University DU QUÉBEC, MONTRÉAL, NOVEMBER 11TH, 2016.

[51] DJERIRI Youcef, MEROUFEL Abdelkader, B. BELABBES and MASSOUM Ahmed, « Three-level NPC voltage source converter based direct power control of the doubly fed induction generator at low constant switching frequency » ; Revue des Energies Renouvelables, Centre de Développement des Energies Renouvelables- CDER, Algérie, Vol.16, No.1, pp.91103, 2013.

[52] GHENNAM Tarak, « Supervision D'une Ferme Eolienne Pour Son Intégration Dans La Gestion D'un Réseau Electrique, Apports Des convertisseurs multi niveaux Au réglage Des Eoliennes à Base De Machine Asynchrone à Double Alimentation », Thèse De Doctorat De l'Ecole Militaire Polytechnique d'Alger 2011.

[53] MEYNARD Thierry. **and A, FADAL Maurice, and N. AOUDA**, « Modelling of multilevel converters » ; IEEE Transaction on Industrial Electronics, Vol.44, No.3, 1997.

.

Abstract:

In recent years, Multiphase machines are increasingly used in high power applications for reasons of reliability and power segmentation. The six-phase induction machine (6PH-IM) was one of such machines. It consists of two sets of identical three-phase windings in the same stator, and supplied by two voltage converters. Several researches are currently directed towards the applications of multilevel converters to improve the performance of control algorithms. This thesis aims to study by simulation the field oriented control (FOC) of a six-phase induction machine driven by two multilevel voltage converters.

Key words:

Multiphase machines, Six phases induction machine (6PH-IM), Field oriented control (FOC),Multilevel power converters.

Résumé:

Ces dernières années, les machines multiphases sont de plus en plus utilisées dans les applications à haute puissance pour des raisons de fiabilité et de segmentation de puissance. La machine asynchrone à six phases (6PH-IM) était l'une de ces machines. Il se compose de deux ensembles d'enroulements triphasés identiques dans le même stator, et alimentée par deux convertisseurs de tension. Plusieurs recherches sont actuellement orientées vers les applications de convertisseurs multiniveaux pour améliorer les performances des algorithmes de contrôle. Cette mémoire vise à étudier par simulation la commande de flux orientée (FOC) d'une machine asynchrone à six phases entraînée par deux convertisseurs de tension multiniveaux.

Mots clés :

Machines multiphases, Machine asynchrone à six phases (6PH-IM), Commande à orientation de flux (FOC), Convertisseurs de puissance multi-niveaux.

الملخص:

في السنوات الأخيرة، يتم استخدام آلات متعددة الأطوار بشكل متزايد في تطبيقات الطاقة العالية لأسباب عدة منها الموثوقية وتقسيم الطاقة. حيث كانت آلة الحث المكونة من ستة أطوار واحدة من هذه الآلات والتي تتكون من مجموعتين من اللفات المتطابقة المكونة من ثلاث أطوار ، ويتم تغذيتها بواسطة محولين للجهد. يتم توجيه العديد من الأبحاث حاليًا نحو تطبيقات المحولات متعددة المستويات لتحسين أداء خوارزميات التحكم. تهدف هذه الأطروحة إلى دراسة عن طريق محاكاة التحكم الموجه ميدانيًا لآلة حث من ستة مراحل مشغلة بمحولين للجهد متعدد المستويات.

كلمات مفتاحية :

آلات متعددة الأطوار, آلة حث ست أطوار, تحكم شعاعي , محولات طاقة متعددة المستويات.